Synthesis and Characterization of Hybrid Al-based Matrix Composites Fabricated by Spark Plasma Sintering

M.Tech. Thesis

By

Yogendra Sharma

Department of Metallurgical Engineering and Material Science

Indian Institute of Technology Indore

June 2023

Synthesis and Characterization of Hybrid Al-based Matrix Composites Fabricated by Spark Plasma Sintering

A THESIS

Submitted in the partial fulfilment of the
Requirements for the award of the degree
of
Master of Technology

By

Yogendra Sharma

Department of Metallurgical Engineering and Material Science

Indian Institute of Technology Indore

June 2023

INDIAN INSTITUTE OF TECHNOLOGY INDORE

Candidate's Declaration

I hereby certify that the work which is being presented in the thesis entitled **Synthesis and Characterization of Hybrid Al-based Metal Matrix Composites Fabricated by Spark Plasma Sintering** in the partial fulfilment of the requirements for the award of the degree of **MASTER OF TECHNOLOGY** and submitted in the **DEPARTMENT OF METALLURGICAL ENGINEERING AND MATERIAL SCIENCE, Indian Institute of Technology Indore,** is an authentic record of my own work carried out during the time period from August 2021 to May 2023 under the supervision of **Dr. Ram Sajeevan Maurya**, Assistant Professor, Department of Metallurgical Engineering and Material Science, Indian Institute of Technology, Indore.

Sharma 1/06/23

Signature of the student (with date)

This is to certify that the above statement made by the candidate is correct to the best of my knowledge.

RSM 01/06/2023

Signature of the Supervisor of M.Tech. Thesis (with date)

Yogendra Sharma has successfully given her M.Tech. Oral Examination held on 25th **May 2023**.

RSM 01/06/2023

Signature of Supervisor of M.Tech. Thesis

Signature of Convener, DPGC

Signature of PSPC Member:

Signature of PSPC Member:

Acknowledgments

I would like to express my heartfelt gratitude and appreciation to the following individuals and organizations who have played a significant role in the successful completion of my M.Tech thesis:

First and foremost, I am deeply grateful to my research supervisor, **Dr. R.S. Maurya** for his invaluable guidance, unwavering support, and expert insights throughout the entire research process. His encouragement, patience, and exceptional mentoring have been instrumental in shaping this thesis. Financial support from the Science and Engineering Research Board (SERB), Government of India (Project No. ECR/2018/000164) is gratefully acknowledged.

I take this opportunity to express my gratitude to **Prof. Sushas S. Joshi**, Director, IIT Indore for providing the essential facilities, valuable guidance, and cooperation.

I am extremely happy to express my gratitude towards PSPC members **Dr. Sumanta Samal** and **Dr. Hemant Borkar** for their guidance and support. I am thankful to **Dr. Ajay Kushwaha,** HOD MEMS for his support and cooperation. I am thankful to all the faculty members of the department of MEMS for their guidance and support.

I would like to acknowledge the assistance provided by the MEMS Department IIT Indore staff and technicians, who generously shared their expertise and resources, making my research endeavours possible.

I would like to express my gratitude to **MHRD, Govt of India** for providing fellowship during my master's studies to carry out this research. Their investment has been instrumental in the successful completion of this thesis.

Finally, I would like to thank all the authors, researchers, and scholars whose work and publications have served as a guiding light for my research. Their contributions have laid the foundation for my understanding of the subject matter.

The completion of this M.Tech thesis would not have been possible without the support, guidance, and contributions of the individuals and organizations mentioned above. I am deeply grateful for their involvement and dedication.

Dedication

This thesis is dedicated to my parents, sisters,
seniors and friends for their constant love,
encouragement and patience.

Abstract

The present paper is based on the fabrication and characterisation of Hybrid AMMC. Moving further, mechanical properties of the fabricated composite materials are also discussed. In the present work, aluminium is taken as the matrix material, and SiC and Al_2O_3 are the ceramic particles taken as the reinforcements. Weight percentage of reinforcements are limited to 10wt%, where combination of percentage of SiC and Al_2O_3 are taken as (8 wt%,2 wt%) and, (6 wt%, 4 wt%) respectively .Fabrication of the composites' samples are done through Powder Metallurgy route. Mechanical milling is done to mix composite powders, and consolidation is done through the Spark Plasma Sintering process. XRD patterns of powders after regular intervals of mechanical milling are discussed. Density of samples consolidated through Spark Plasma Sintering came out more than 97% as opposed to Hot Press, where maximum density achieved was 89%. EDS mapping of composite samples is utilized to show the kind of distribution of reinforcement particles in the aluminium matrix. Results showed that hardness and compressive strength of aluminium is improved by mixing SiC and Al_2O_3 particles. Study based on the fretting wear of the AMMC samples is also discussed, where characteristics such as the coefficient force and the friction force is discussed. Coefficient of friction graphs for different compositions shows that samples with lesser holding time and higher percentage of SiC in SPS consolidation shows higher COF values. Study of the wear surface based on the SEM images is done after fretting wear of composite samples at two different loads of 20N, 30N with the frequency of 10 Hz, with displacement amplitude of 0.2 mm. Maximum compression strength of 492 MPa and 476 MPa was achieved for Al composites containing reinforcemnt of (8 wt% SiC, 2 wt% Al_2O_3) and (6 wt% SiC, 4 wt% Al_2O_3).

Table of Contents

List of Figures

List of Tables

Chapter 1

Introduction

The foundational ideas needed to comprehend the information that is provided in this thesis are introduced in this chapter. The summary of the present composite research landscape, which inspired us to conduct this study, comes first. The following section provides an overview regarding it.

The material under discussion is Hybrid Metal Matrix Composites. The next section addresses the manufacturing processes used to create MMCs and the rationale for the choice of powder metallurgy, which is then followed by a review of the workings of the various machines employed in the powder metallurgy process.

1.1 General Overview

Around 4.6 metric tonnes of carbon dioxide are emitted annually by a typical passenger automobile. Depending on the fuel type, fuel efficiency, and annual miles of a vehicle, this number may vary.

Automobiles also emit methane (CH_4), nitrous oxide (N_2O), and hydrofluorocarbons from leaking air conditioners in addition to carbon dioxide (CO_2). Although these gases produce less emissions than CO_2, they yet have a far greater potential to contribute to global warming than CO_2.

Automotive OEMs will be able to cut these emissions, thanks in large part to light-weighting, which saves (on average) 8.5g of CO_2 per 100km. A light-weighting plan is necessary for all cars to cut emissions, not just those with internal combustion engines. Manufacturers of electric vehicles (EVs) are focused on reducing weight as they work to extend the range of a single

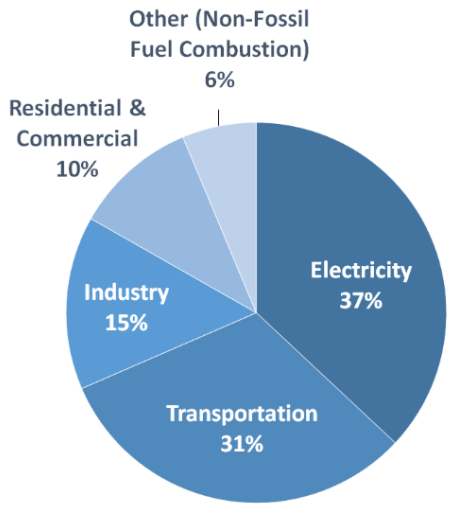

Figure 1.1: Emissions of Greenhouse gases from different sources.

charge.

Engineers have been searching for methods to reduce component and assembly weight for decades in order to produce greener and more cost-effective products. Products can frequently be produced to match performance criteria with less resources by using more optimal options, or eliminate specific materials entirely, as production processes and raw materials evolve.

In the past, the automobile and aerospace industries prioritised lightweighting to maximise fuel efficiency. As a result, current electric vehicles' battery ranges are improving, while aeroplane payloads are rising. Lightweighting is increasingly a common objective for producers and designers of consumer goods, medical equipment, and much more as other industries move towards greener, more efficient, and more pleasant solutions.

Aluminium and magnesium are two of the main metals that will enable weight loss. Aluminium weighs around one-third of what steel does, whereas magnesium is the lightest structural metal and is also widely available. Both metals are already widely used in automobiles.

These material advancements, however, must compromise safety. For automotive parts, ductile strength, structural rigidity, corrosion resistance, and temperature resistance are still essential qualities. These components are far from ideal on their own.

The aluminum's physical characteristics show this to be the case. Aluminium can be fairly fragile when used alone. Thus, we use aluminium alloys and aluminium composites for better strength and improved wear and corrosive properties for various applications.

1.2 Composites

The materials needed for many of our current technology must include odd mixes of qualities that the traditional metallic alloys, ceramic materials and polymers are unable to meet. Atleast two distinct materials from the previously mentioned categories—metals, polymers and ceramics —combine to form a composite.

In addition to incorporating the greatest qualities of each of the component elements, the prime objective of a composite is such that it should attain a set of properties that no single material can demonstrate. There are many various types of composite materials that can be combined with metals, ceramics, and polymers.

Figure 1.2: Graphite particle reinforced aluminium composite.

The composites' properties depend on the properties of the constituent phases, their relative weight or atomic percentages, and the geometry of the reinforcemnets, which in this frame of reference refers to the shape as well as their size, distribution, and orientation of the particles.

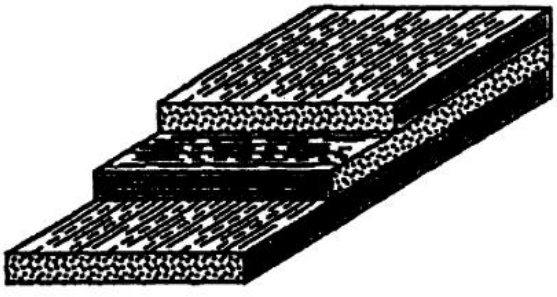

Continuous fibers

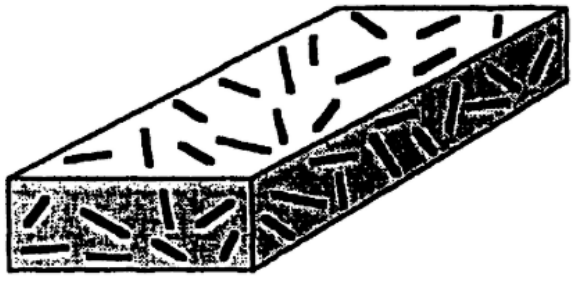

Discontinuous Fibers, Whiskers

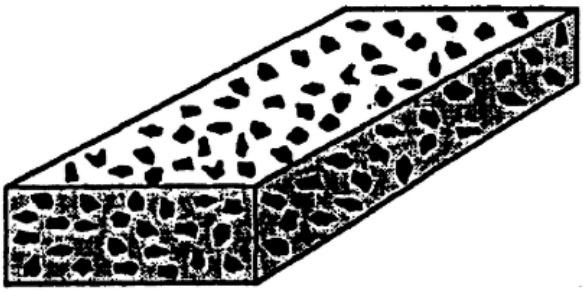

Particles

Figure 1.3: Schematic of fiber and particle reinforced composites.

Many composites consist of simply two phases; one is referred to as the matrix, that is continuous and it surrounds the other , which is frequently called the reinforcement or dispersed phase.

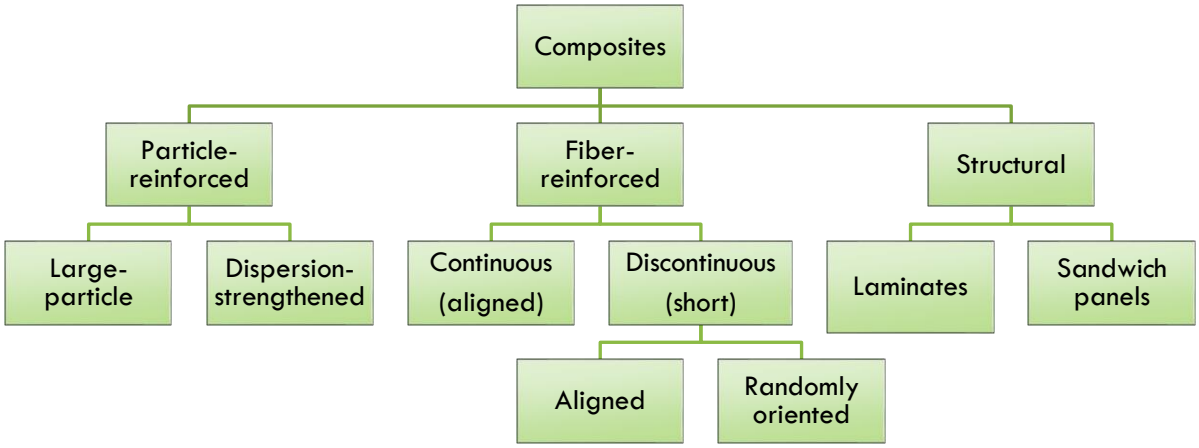

Figure 1.4: Classification of Composite Materials.

Particle-Reinforced Composites

The two subcategories of particles reinforced composites are large particle and dispersion strengthened composites. Based on the method for reinforcing or strengthening, these are distinguished from one another.

When a particle matrix interaction is described as "large," it means that it cannot be understood at the atomic or molecular level and must instead be understood using continuum mechanics. The particulate phase of the majority of these composites is stiffer and harder than the matrix. The mobility of the matrix phase tends to be restrained around each of these reinforcing particles. Basically, some of the applied stress is passed from the matrix to the particles, which are capable of supporting a minimal amount of the load.

1.2.2 Fiber -Reinforced Composites

The most significant composites in terms of technology are those in which the dispersed phase takes the shape of a fibre. In addition to the characteristics of the fibres, a fibre reinforced composite's mechanical properties also depend on how efficiently the matrix phase transmits applied loads to the fibres. For the composite material to be effectively strengthened and stiffened, a certain critical fibre length is required.

$$l_C = \frac{\sigma_f^* d}{2\tau_C}$$

For a range of glass and carbon fibre matrix combinations, this critical length, which varies between 20 and 150 times the fibre diameter, is on the order of 1 mm.

Continuous fibres are those for which $l >> l_c$ (typically); discontinuous or short fibres have lengths below this.

1.3 Metal Matrix Composites

Metal matrix composites (MMCs), like other composite materials, are composed of at least two physically and chemically distinct phases that are spread to provide properties that are not feasible with each phase alone. Typically, a metallic matrix contains two phases, such as a fibers or particles. For superconducting magnets, continuous $A1_20_3$ fibre reinforced A1 matrix composites; Tungsten carbide (WC)/cobalt (Co) particulate composites, Nb-Ti filaments in a copper matrix, used as cutting tools and oil drilling inserts, and Sic particle reinforced A1 matrix composites used in aerospace, automotive, and thermal management applications are a few examples.

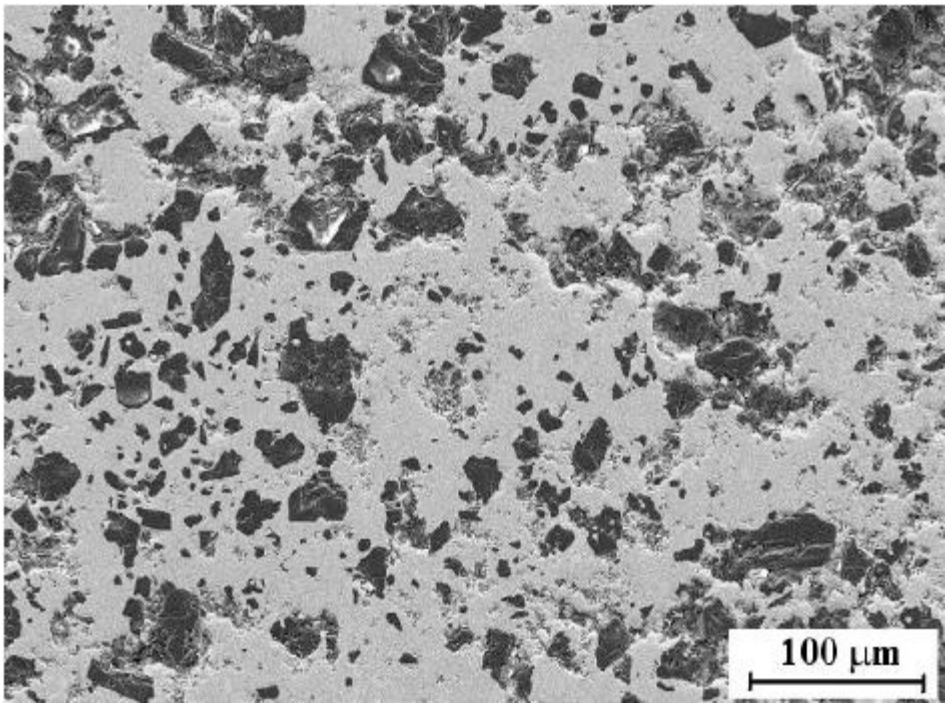

Figure 1.5: SEM image of area of composite microstructure [23].

"Why metal matrix composites?" Response to the query may be classified into 2 categories:

(i) Benefits over unreinforced metals in and (ii) advantages over other composites for example, polymer matrix composites (PMCs). The benefits of MMCs for metals include the following:

- Stronger strength-to-weight ratio results in significant weight savings.

- extraordinary dimensional stability (for instance, compare SiC/Al to Al)
- Greater increased temperature stability, or resistance to creep
- Improved cyclic fatigue properties noticeably

1.3.1 Characteristics of MMCs:

Of course, improved strength and stiffness are among the elements influencing the evolution of metal matrix composites. There are other qualities that could be just as desirable. We may use the capacity to regulate heat expansion in applications requiring electronic packaging as examples. In general, one may lower the composite's coefficient of linear thermal expansion by adding ceramic reinforcements. In some applications, thermal and electrical conductivity qualities can be crucial. It is obvious that superconductors require superconducting properties. The matrix holds the microscopic superconducting filaments together as well as acting as a high thermal conductivity medium in the event of an unintentional quench.

Wear resistance is another crucial quality that might be quite valuable (for example, in Tungsten Carbide/Co composites used in cutting tools or oil drilling inserts and SiC_p/Aluminium rotor in brakes.

1.3.2 Reinforcements:

Continuous fibres, short fibres, whiskers, or particles can all be used as reinforcement in metal matrix composites. The aspect ratio is the variable that enables us to differentiate between these several reinforcement types. The ratio of a fibre, particle, or whisker's length to its diameter (or the thickness) is known as the aspect ratio. As a result, completely equiaxed particles have an aspect ratio of about 1, but continuous fibres have an aspect ratio that is almost infinite. Some significant reinforcing materials that come in various forms are listed in Table 1.1. Ceramic reinforcements have a high elastic modulus, high strength, and high temperature capacity.

However, the cost of continuous ceramic fibres is likewise higher than that of ceramic particle reinforcement.

Table 1.1: Important Reinforcements for MMCs

Type	Aspect Ratio	Diameter, μm	Examples
Particle	1-4	1-25	SiC, Al_2O_3, BN, B_4C, WC

Short fiber or whiskers	10-1000	1-5	C, SiC, Al_2O_3, SiO_2
Continuous fibers	>1000	3-150	C, SiC, Al_2O_3, B, W, Nb-Ti, Nb_3SN

1.4 Processing:

Processes in the liquid, solid, or gaseous states can be used to create metal matrix composites. We discuss various significant MMC fabrication processing methods in this chapter.

1.4.1 Liquid State Processing

A liquid metallic matrix can be incorporated into or combined with the reinforcement to create metal matrix composites. Using a liquid phase processing method provides a number of benefits. Those include the near net-shape (in comparison with solid state techniques like diffusion bonding or extrusion) and quicker processing rates, as well as the typically low melting temperatures of most light metals, including A1 and Mg. There are four main categories into which the most popular liquid state processing methods can be divided:

Stir Casting: This entails mixing liquid aluminium melt with ceramic particles and letting the combination set up. Here, it's essential to have liquid aluminium alloy melt and the particle reinforcement well-wetted. The stir-casting technique or vortex technique is the most basic and widely utilised method. The vortex approach includes introducing pre-treated ceramic particles into the revolving impeller's molten alloy vortex. According to Lloyd (1999), the vortex-mixing process was first created by Surappa & Rohatgi (1981) for the manufacture of ceramic particle dispersion aluminium matrix composites. Later, a number of aluminium businesses improved and altered the procedure, which is now used to create a number of AMCs on a large scale.

Particularly during the melt and afterwards during solidification, microstructural inhomogeneity can lead to particle agglomeration and sedimentation. Because of the interplay between moving solid-liquid interfaces and suspended ceramic particles during solidification, inhomogeneity in the distribution of reinforcement in these cast composites may potentially be a concern. Generally speaking, a variety of molten aluminium alloys can contain up to 30% of ceramic particles with a size range of 5 to 100 m. The melt-ceramic particle slurry may be poured immediately into a

formed mould before solidification is complete, or it can be allowed to harden into billets or rods so that it may be warmed to slurry form for processing by methods such die or investment casting.

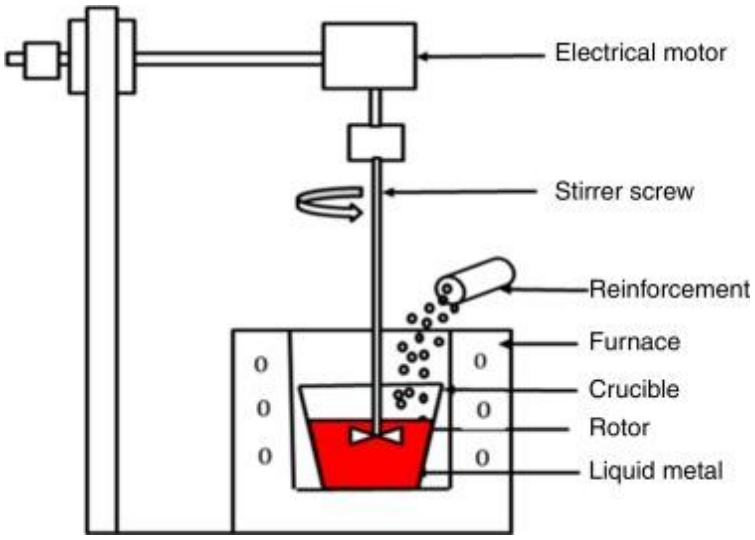

Figure 1.6: Schematic diagram of the fabrication of MMCs by Stir casting technique [24].

- **Pressure Infiltration process:** This technique involves liquid infiltration of a fibrous or particulate preform with pressure being continuously applied. This method suits best for intricately formed components, localised or selective reinforcing, and situations where output speed is crucial.
- **Spray co-deposition:** Here**,** in this method, ceramic particles are injected into the spray stream together with the liquid metal to create a granulated mixture of composite particles. After that, the composite particles are solidified using a different effective method, for example- hot pressing, extrusion, forging, etc.

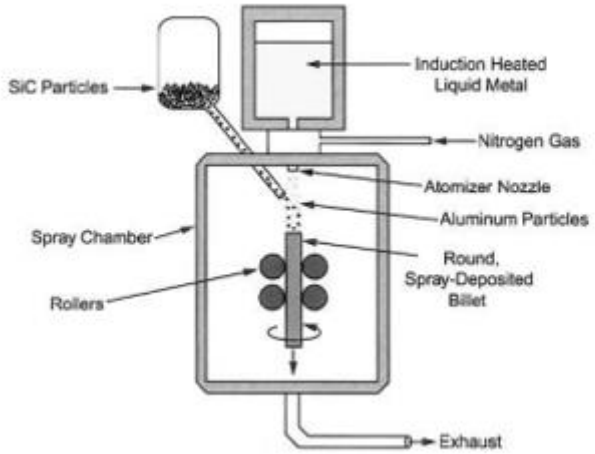

Figure 1.7: Spray co-deposition of Sic particles and A1 liquid droplets, to form composite particles [25].

1.4.2 Solid State Processing:

The one of the difficulties is regulating reinforcement distribution and creating a consistent matrix microstructure is the primary disadvantage of liquid phase approaches (Michaud, 1993). Furthermore, due of the high temperatures required in liquid state processing, undesirable interfacial interactions between the reinforcement and matrix are likely to take place. The composite's mechanical characteristics may suffer as a result of these processes. Based on powder metallurgy methods, solid phase procedures are most frequently used. Because of the reason of the simplicity of mechanical milling and the efficiency of densification, these usually include discontinuous reinforcements. The metal and ceramic powders are combined, isostatically cold crushed, then heated to achieve their maximum density. After that, the completely dense compact often goes through a secondary process like extrusion or forging.

1.4.2.1 Powder Metallurgy Processing:

Powder metallurgy is a process of making metal components by using powders of various metals. In this process, metal powders are mixed, pressed, and sintered to produce a finished product. The following steps are used in the powder metallurgy process:

- Powder Production: The first step is the production of metal powders. These powders are often made by atomization, which involves spraying molten metal through a nozzle and

allowing the droplets to cool and solidify. Electrolysis, chemical reduction, and grinding are other methods used for powder production.

- Powder Blending: Next, the metal powders are blended to achieve the desired composition. This step is essential because different types of powders may have different properties, such as particle size, shape, and purity.
- Compaction: The blended powder is then loaded into a die and pressed to form a compact with a specific shape. The pressing is done by applying high pressure to the powder particles in a die to create a green sample.
- Sintering Process: The green compact is then subjected to heat treatment in a furnace, where the powder particles coalesce through diffusion, and the compact is transformed into a dense, solid product. The sintering process includes heating the green compact to the temperature below its melting point to cause the metal particles to bond. The sintering temperature, time, and atmosphere are chosen to optimize the properties of the final product.

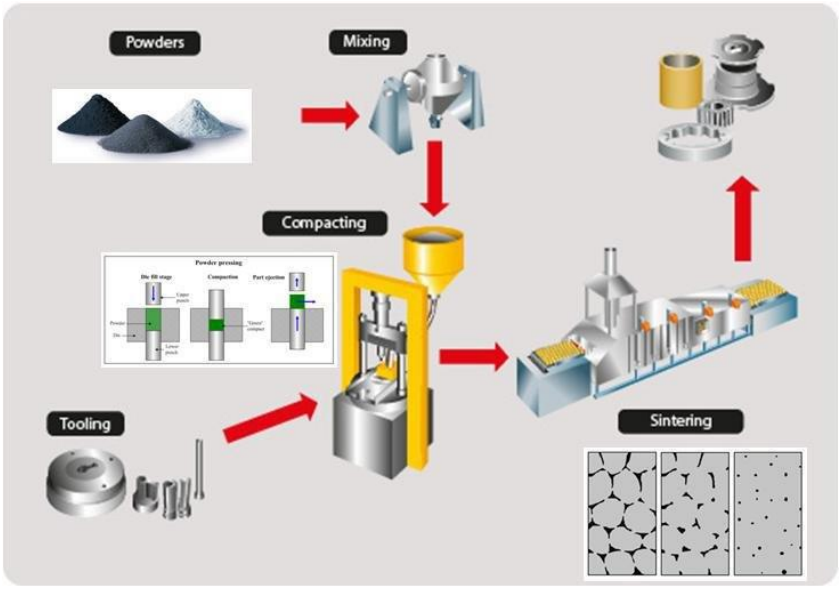

Figure 1.8: Stages of Powder EMtallurgy Process[26].

1.4.2.2 Diffusion Bonding:

The diffusion bonding or foil-fibre-foil methodor the evaporation of large layers of aluminium on the fibre surface are the two basic methods for creating mono filament-reinforced aluminium

matrix composites. By using the foil-fibre-foil technique and diffusion bonding, 6061 Al-boron fibre composites have been created. However, Ti-based fibre reinforced composites are more frequently created using this method. The procedure is time-consuming, and it is challenging to achieve high fibre volume fraction and homogenous fibre dispersion. Complex forms and components can't be produced with this approach.

1.4.2.3 Physical Vapour Deposition:

Continuous transit of the fibre through the zone of high partial pressure of the metal to be deposited is required for the process, where condensation occurs to generate a rather thick coating on the fibre. An intense electron beam is focused onto the end of a solid bar feed stock to create the vapour. Deposition rates typically range from 5 to 10 m/min. The coated fibres are typically assembled into an array or bundle before being compressed in a HIP or hot press operation to finish composite production. By using this method, composites with a volume fraction of up to 80% and homogenous fibre dispersion may be created.

1.5 Machines used in fabrication of HAMMC :

1.5.1 Planetary Ball Mill

Planetary Ball mill is one of the popular ball mills in which a few hundred grams of powders can be milled at once. One of the well-liked types of ball mills that can grind a few hundred grammes of powder at once is the planetary ball mill. The planet like movement of its vials is where the planetary ball mill gets its name. These are stacked on a revolving support disc and rotate around their own axes thanks to a unique driving system. The spinning support disc and the rotating vials' centrifugal forces both exert pressure on the vial contents, which are made up of the grinding balls and the material to be ground. The centrifugal forces alternatively operate in like and opposing directions because the vials and the supporting disc revolve in opposite directions. This causes the grinding balls to run down the inside wall of the vial, which is what generates the friction effect. The grinding balls then lift off and move freely through the inner chamber of the vial, slamming against the opposing inside wall - the impact effect - as the material is ground. There are various parameters on which milling process is based. Following are the prime ball milling parameters that needs to be taken care of:

- Ball to Powder ratio

- Milling Speed
- Milling Time
- Process Control Agent

Figure 1.19: Planetary Ball Mill (PM200, Retsch, Germany)

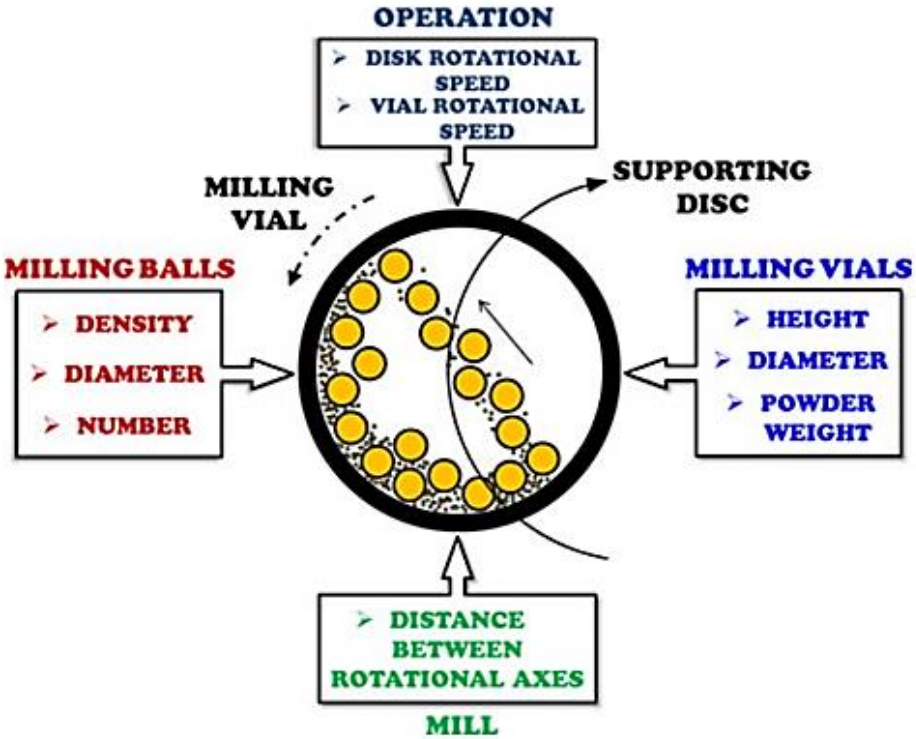

Figure 1.10: Schematic of Ball Milling Process n Planetary Ball Mill.

1.5.2 Spark Plasma Sintering Machine (SPS)

In order to consolidate and densify powder materials into solid structures, Spark Plasma Sintering (SPS), an advanced powder metallurgy process, applies high temperatures and pressure. The SPS machine is a piece of highly specialised machinery utilised in this procedure.

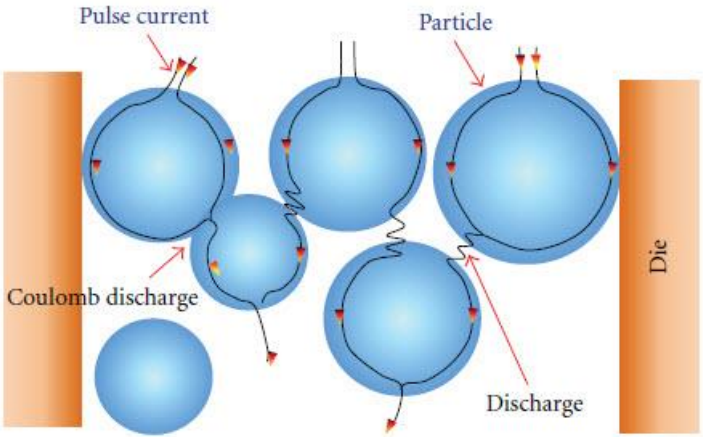

Figure 1.11: DC pulse current flow

A cylindrical chamber with the ability to endure high temperatures and pressures is part of the SPS machine. The chamber has two electrodes—the upper and lower electrodes—made of highly conductive materials like graphite or copper.

SPS typically involves four basic steps. In the first step, vacuum is created and gases are expelled. The second stage involves applying pressure, the third stage involves resistive heating, and the fourth stage involves cooling. A local high-temperature state of several to ten thousand degrees centigrade is temporarily formed when a spark discharge arises in a gap or at the point of contact between the particles of a material.

In comparison to conventional sintering methods, the process takes just a few minutes to complete, and the finished product has higher density,

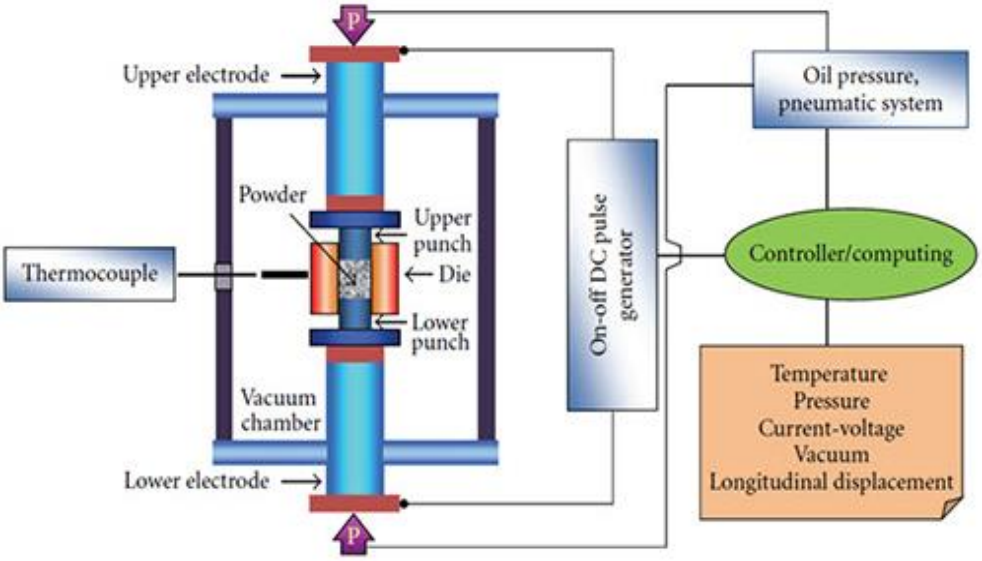

Figure 1.12: Schematic Diagram of SPS process.

a finer microstructure, and better mechanical qualities. The typical heating speeds in ordinary furnaces are 5 to 8°C/min, with a maximum of 10°C/min.

Therefore, it will typically take 2 to 4 hours or longer to reach a temperature of 1200°C, but with SPS, heating rates surpassing 300°C/min are easily achieved; as a result, a temperature of 1200°C may be reached in just 4 minutes.

In comparison to traditional sintering techniques, the SPS machine offers a number of benefits, including faster processing times, superior sintering parameter control, the capacity to sinter complicated forms, increased product uniformity, and lower energy usage.

Figure 1.13: Spark Plasma Sintering Machine (SPS 625, Fuji Electronic Industrial Co. Ltd.).

Numerous industries, including the aerospace, automotive, medicinal, and energy sectors, have used the SPS machine. Advanced materials including ceramics, composites, intermetallics, and nanostructured materials may all be produced with this process. Due to improvements in research and development efforts, the technology is anticipated to become increasingly significant in the upcoming years.

Chapter 2

Literature Review

In the last few decades, there has been intense research being done in the field of metal matrix. composites that also led to many practical applications of metal matrix composites (MMCs). Aluminium being among lightest metals that is available in large amount and economically cheap, has been the choice for replacement of conventional materials like steel. Owing to its high specific strength as well as high specific modulus, aluminium alloys are preferred over conventional metals, but they have limited mechanical and wear properties [2, 3]. MMCs are a group of materials where light metals such as aluminium as a matrix is reinforced with certain ceramic particles. In the form of Aluminium matrix composites (AMMCs), low density along with higher stiffness, higher compressive strength, higher wear resistance and thermal expansion coefficient is achieved as compared to unreinforced aluminium. The tensile and compressive strength of some AMMCs has been found to be increased more than 40% as compared to pure aluminium [1]. They have uses in the automotive, aviation, space, defence, energy, electronics, and precision mechanics industries because of their unique features [4, 5].

In this literature review, we will explore some of the recent research studies on aluminium HMMCs, their properties, and potential applications.

2.1 Influence of reinforcing particles over mechanical and tribological properties

The properties such as tribological and mechanical properties of aluminium HMMCs are highly dependent on the type, size, and weight percentage of the reinforcing materials. The addition of reinforcing materials can also improve the thermal conductivity and tribological characteristics of the composite. However, the addition of reinforcing materials can also have a negative impact on the ductility and toughness of the composite.

1. K. Ramanathan et al. (2019) investigated the mechanical properties of aluminium-based hybrid composites reinforced with silicon carbide and carbon fibers. The results showed that the addition of carbon fibers improved the tensile strength and hardness

of the composites, while the addition of silicon carbide enhanced their compressive strength and wear resistance.

2. Nagarajan et al. (2018) studied the tribological behaviour of aluminium hybrid composites reinforced with silicon carbide and graphite. The results indicated that the addition of graphite improved the wear resistance and reduced the coefficient of friction of the composites.
3. K. Sankaranarayanasamy et al. (2017) investigated the mechanical properties and microstructure of aluminium-based hybrid composites reinforced with silicon carbide and alumina. The results showed that the addition of alumina improved the hardness and wear resistance of the composites, while the addition of silicon carbide enhanced their compressive strength.
4. K. Singh et al. (2016) studied the mechanical and tribological properties of aluminium hybrid composites reinforced with silicon carbide and carbon nanotubes. The results showed that the addition of carbon nanotubes improved the hardness, tensile strength, and wear resistance of the composites.
5. S. B. Kadam et al. (2015) investigated the mechanical properties and wear behaviour of aluminium hybrid composites reinforced with silicon carbide and titanium carbide. The results indicated that the addition of titanium carbide improved the wear resistance and reduced the coefficient of friction of the composites.
6. M. Ashok Kumar et al. (2014) studied the mechanical properties and microstructure of aluminium hybrid composites reinforced with silicon carbide and fly ash. The results showed that the addition of fly ash improved the hardness and wear resistance.
7. In a study by Ghosal et al. (2020), aluminium hybrid composites reinforced with silicon carbide and fly ash were fabricated using stir casting. The results showed that the addition of fly ash improved the mechanical properties of the composite, including the tensile strength, hardness, and wear resistance.
8. In a study by Kalaiselvan et al. (2020), aluminium hybrid composites reinforced with aluminium oxide and graphene nanoplatelets fabricate by PM route, showed that the addition of graphene nanoplatelets improved the mechanical properties of the composite, including the tensile strength, hardness, and wear resistance.

9. In a study by Singh et al. (2021), aluminium hybrid composites reinforced with titanium and carbon nanotubes were fabricated using stir casting. The results showed that the addition of carbon nanotubes improved the mechanical properties of the composite, including the tensile strength, hardness, and wear resistance.

2.2 Role of SiC and Al_2O_3 as reinforcements

Based on the literature review of various composites reinforced with ceramic particles, following conclusions can be drawn:

- Al_2O_3 imparts high tensile strength, high hardness, and high wear strength.
- When we increase the SiC composition in Al composites, it also enhances the hardness, ultimate stress and density.
- As Compared to Al_2O_3, SiC enhances the tensile strength by a greater value.
- Instead of using single reinforced composites, hybrid composites showed better mechanical properties.

Table 2.1: Hardness value of Al composites [27].

Composition	Observed Value of Hardness in BHN	Test Parameters
Al (100%)	38	Indenter Ball size: 5mm Load: 250 kg
Al+Al_2O_3 (96 wt%+4 wt%)	45	
Al+Al_2O_3 (92 wt%+8 wt%)	61	
Al+Al_2O_3 (88 wt%+12 wt%)	70	
Al+Al_2O_3+SiC (92 wt%+4 wt%+4 wt%)	82	
Al+Al_2O_3+SiC (90 wt%+5 wt%+5 wt%)	87	
Al+Al_2O_3+SiC (88 wt%+6 wt%+6 wt%)	93	

Data mentioned in Table 2.1 and Table 2.2 shows the variation in mechanical characteristics of composite material with variation in weight percentage of reinforcements (SiC and Al_2O_3).

Table 2: Yield strength and elongation data reported by Ravikumar et. al[28].

Material's Composition	Test Parameters		
	Yield Strength (MPA).	Ultimate Tensile Strength (MPa).	% Elongation in 50 mm Gauge Length.
Al (100%)	33	62	22.50
$Al+Al_2O_3$ (96 wt%+4 wt%)	38	67	14.00
$Al+Al_2O_3$ (92 wt%+8 wt%)	45	73	13.50
$Al+Al_2O_3$ (88 wt%+12 wt%)	50	80	14.00
$Al+Al_2O_3$+SiC (92 wt%+4 wt%+4 wt%)	61	86	9.00
$Al+Al_2O_3$+SiC (90 wt%+5 wt%+5 wt%)	67	90	11.50
$Al+Al_2O_3$+SiC (88 wt%+6 wt%+6 wt%)	70	92	12.00

2.3 Spark Plasma Sintering Process and Parameters

There are several methods used to fabricate aluminium HMMCs, including stir casting, powder metallurgy, and infiltration. Stir casting is the most widely used method due to its simplicity and low cost. In this method, the reinforcing materials are added to the molten aluminium and stirred to distribute the particles evenly. Powder metallurgy involves mixing the aluminium powder with the reinforcing materials, followed by compacting and sintering.

Difference in the density of the ceramic particles and aluminium can result in non-uniform distribution of ceramic particles in the aluminium matrix in liquid state processing techniques.

Powder metallurgy route, which involves mixing the reinforcement particles and Al powder followed by sintering, produces AMMCs having uniform distribution and process is also not affected by the wettability of the reinforcement particles and Al [6, 7].

Due to its remarkable advantages over traditional methods, spark plasma sintering (SPS), which is characterised by rapid heating and cooling during the sintering process, has attracted a lot of interest recently. Better inter-particle bonding is achieved in a shorter amount of time with SPS due to the generation of plasma waves, spark impact pressure, and application of high consolidation pressure [8, 9].

The spark discharge produced during the first stage of sintering results in a localised rise in temperature on the powder particle surfaces, which causes the majority of oxides to evaporate and expose clean metal surfaces, creating the diffusion channel. Diffusion phenomena is hence more intense and activated at a lower temperature.

The SPS process allows for sintering temperatures as low as 300 °C and powder heating rates of up to 1000 °C/min. Thus, samples with high density can be consolidated from composite powders in few minutes via Spark Plasma Sintering.

In the past few years, several AMMCs has been successfully fabricated using SPS that includes Al-CNT [10, 11], Al-SiC [12-16], Al-Al2O3 [17], Al-B4C [18], Al-ZrB2 [19].

By using high-energy ball milling and spark plasma sintering at 500 ℃ with a heating rate of 300 ℃/min and an 8-min cycle, Budha et al. [21] created 5083 powdered aluminium alloy-SiC nanocomposites. Similar to how Li et al. [22] did it, they used a planetary ball mill to combine AA6061 powders with different SiC volume fractions in a WC vial. Then, using the SPS technique, the composites were created using compaction pressure of 50 MPa and a heating rate of 50oC/min. The sintering process was place at 560 ℃ for 3 minutes.

2.4 Research Gap

Despite significant advancements in the field of hybrid aluminium metal matrix composites, there still exists a research gap in understanding the effect of multiple parameters on the mechanical properties of these composites. Such parameters include the selection of different reinforcements, processing technique, temperature, size, orientation, and distribution of reinforcements, among others. Another aspect that requires further attention is the evaluation of the tribological behavior of these composites, which can play an essential role in their practical applications. Moreover, there is still limited research on the production of these composites using eco-friendly and cost-

effective techniques. Therefore, conducting further research in these areas can enhance the understanding of the behavior of hybrid aluminium metal matrix composites, enabling their potential applications in various industries, including automotive, aerospace, and marine, among others.

Chapter 3

Objectives

The motive of the work is to make MMC with aluminium as the matrix material with the help of modern sintering techniques like Spark Plasma Sintering process using various weight percentages of SiC and Al_2O_3 particles. Due to the strengthening process, which includes interactions between the particles and dislocations within the matrix, as with precipitation hardening, the presence of SiC and Al2O3 as reinforcements in the matrix aids in the creation of materials with better mechanical characteristics. Because the dispersed particles are selected to be inert to the matrix phase, the strengthening is also maintained at high temperatures and for lengthy periods of time. The points mentioned below were the objectives of the research work:

- Composition Selection of Hybrid Aluminium Composite
- Synthesis of Al-based composite through Powder Metallurgy
- Optimization of Ball Milling and Sintering Parameters
- Mechanical Milling of Powders
- Consolidation of Ball-milled Powder
- Characterization and Microstructure Evaluation of Ball-milled Powder and Consolidated sample
- Mechanical Properties Evaluation of Consolidated Sample

Consolidation of two chosen composition is also done on varying the holding time during sintering process via SPS. Composite powders were sintered at temperature 550^o C at pressure of 50 MPa with varying holding time of 10 min and 15 min. Comparison of compression strength, hardness and wear properties of the sintered composites is done.

Chapter 4

Methodology

Composite Powders was prepared with compositions Al (90 wt%)–SiC (8 wt%)–Al_2O_3 (2 wt%) and Al (90 wt%)–SiC (6 wt%)–Al_2O_3 (4 wt%) by blending elemental powders of Al (99%, 325 mesh), SiC (>99%, 200 mesh), Al_2O_3 (>99%, 325 mesh) procurred from SRL chemicals, Sigma-Aldrich.

Mechanical milling of powders was carried out in a planetary ball mill (PM200, Retsch.) using hardened steel balls and vials with ball to powder. weight ratio of 10:1, and the disc rotational speed of 300 rpm.. The milling cycle was set for 15 minutes, followed by cooling for 15 minutes. Direction of rotation was changed after every 15 minute milling cycle for better mixing. 80 ml Toluene was added as a process. control agent (PCA) to check the excessive cold welding leading to powder clustering, and toluene helps to prevent oxidation as well. The milled powders were stored in glass bottles inside a vacuum dessicator to avoid oxidation.

Consolidation of the milled powder were carried out using spark plasma sintering process(SPS 625, Fuji Electronic Industrial Co. Ltd., Japan) with the help of tungsten carbide die and punches of 15 mm diameter. The milled powders of both the compositions were sintered at 550^o C and 50 MPa for 10 minutes and 15 minutes with a heating rate of 100^o C. Abbreviations has been used for both the compositions sintered at different sintering parameters and listed in Table 4.1.

Table 4.1: Abbreviations for both compositions sintered at different holding time of 10 min and 15 min.

Sample Composition	**Abbreviations**	**Holding Time**
(Al-SiC 8 wt%-Al_2O_3 2 wt %)	S 1-10	10 min
(Al-SiC 8 wt%-Al_2O_3 2 wt %)	S 1-15	15 min

(Al-SiC 6 wt%-Al_2O_3 4 wt %)	S 2-10	10 min
(Al-SiC 6 wt%-Al_2O_3 4 wt %)	S 2-15	15 min

Microstructural phase analysis of the milled powders and consolidated samples was performed by XRD (3rd generation Empyrean, Malvern Panalytical X-ray Diffractometer) with CuKα (λ=1.54 Å) radiation in 2θ range of 20º to 90º for both the compositions. Scanning Electron Microscope (JEOL-JSM-6480LV) with 15 kV voltage was used to study the particle size and morphology of the milled powders collected at different milling intervals and particle bonding in case of sintered samples. Microhardness of the consolidated samples was studied using Vickers microhardness tester (Conation, Semi-Automatic Microhardness Tester) using diamond indenter with square base. Microhardness test was done at a load of 100 gm with dwell time of 20 seconds. Average of atleast 10 indentations were takenfor estimating the hardness.

Tribological study of the consolidated samples was done by performing fretting wear tests. Samples of cuboidal shape and edge thickness of 5mm were made for the test. The wear tests were conducted at loads of 20 N and 30 N, frequency of 10 Hz and amplitude of 0.2 mm. Samples for compression test were cut from the sintered samples using wire EDM with diameter 2.8 mm and height of 4.9 mm and hence, maintaining the aspect ratio of 1.75. The compression tests were performed at a strain rate of $5 \times 10^{(-4)}$ /s.

Chapter 5

Results and discussion

5.1 Microstructural phase analysis of milled Powders

XRD patterns of mechanically milled composite powders of both the compositions are shown in figures 1a and 1b. As seen in Figs. 1a and 1b, 20 h milled powder displays a significant peak widening in contrast to 1 h milled composite powder. XRD peak broadening (Fig. 1a and 1b) slowed down after 10 hours of milling. Internal structural refinement, including changes in crystallite size, lattice microstrain, and lamellar separation between particles, increases logarithmically with milling duration. As a result, reduced peak intensity loss was seen across longer periods of time. It is evident from the XRD data that no new phase development is seen throughout the milling process.

In both the cases, the deformation mechanism for the compositions remains the same. Aluminium being the soft metal, powder particles gets flattened and form cold welds by the impact of hardened steel balls, making layered composite powder particles and brittle particles of SiC and Al_2O_3 tends to become occluded by aluminium. Work hardened powder particles get fractured along with the cold welding. Ultimately, a refined and homogenised microstructure is obtained with the same initial composition.

Average crystallite size is also calculated with the help of XRD peaks using Scherrer equation. Here, peak broadening helps in determining reduced crystallite size.

$$D = \frac{k\lambda}{\beta \cos \theta} \qquad \text{Equation (1)}$$

Where λ is the X-ray wavelength, β is the peak width, K is a constant (often 1), and θ is the scattering angle.

Figure 5.1: XRD patterns of milled powders for(a) composition 1 (Al-SiC (8 wt%)-Al_2O_3 (2 wt%)) and (b) composition 2 (Al-SiC (6 wt%)-Al_2O_3 (4 wt%)) at different intervals.

a

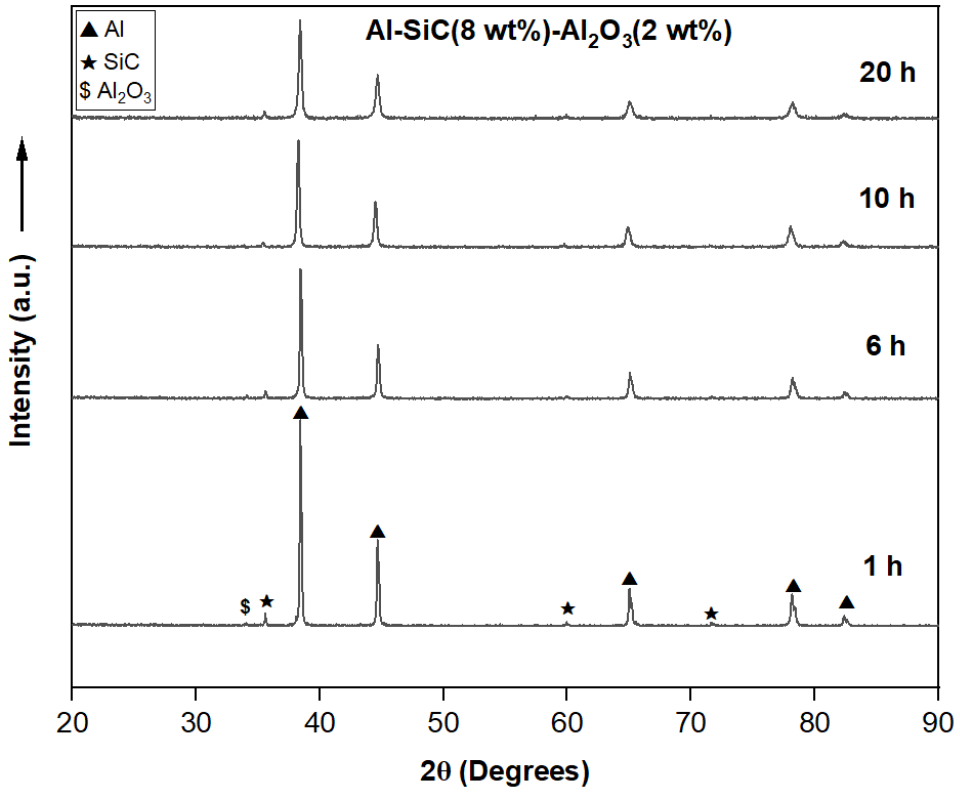
▲ Al
★ SiC
$ Al2O3
Al-SiC(8 wt%)-Al2O3(2 wt%)
20 h
10 h
6 h
1 h
Intensity (a.u.)
2θ (Degrees)
20
30
40
50
60
70
80
90

b

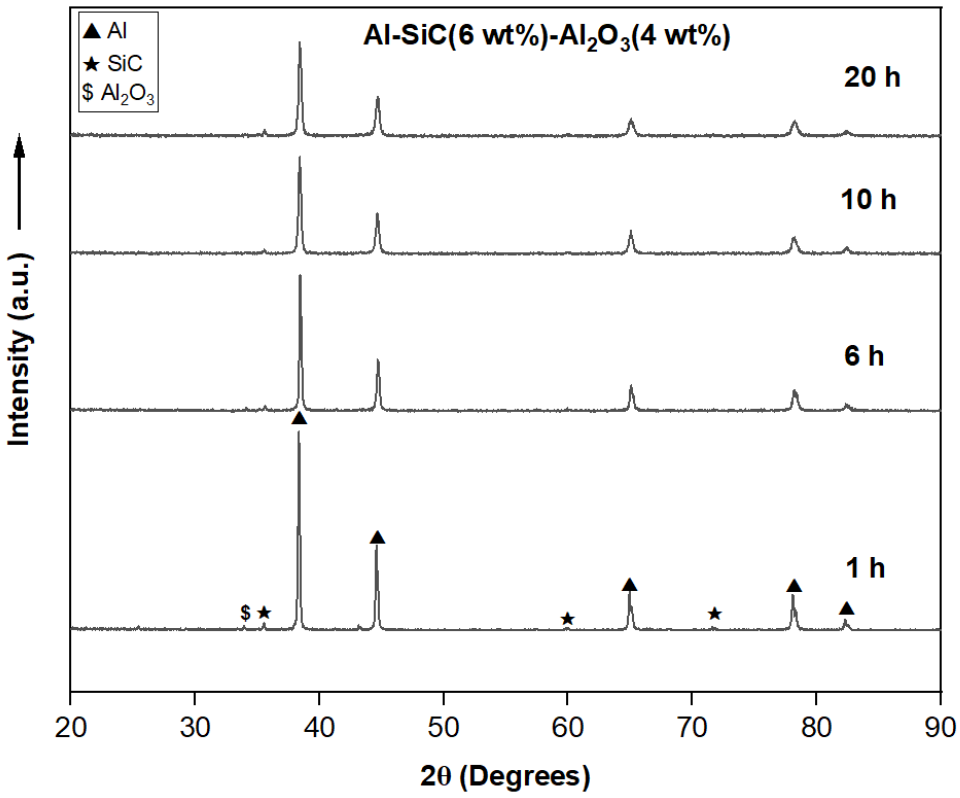
▲ Al
★ SiC
$ Al2O3
Al-SiC(6 wt%)-Al2O3(4 wt%)
20 h
10 h
6 h
1 h
Intensity (a.u.)
2θ (Degrees)
20
30
40
50
60
70
80
90

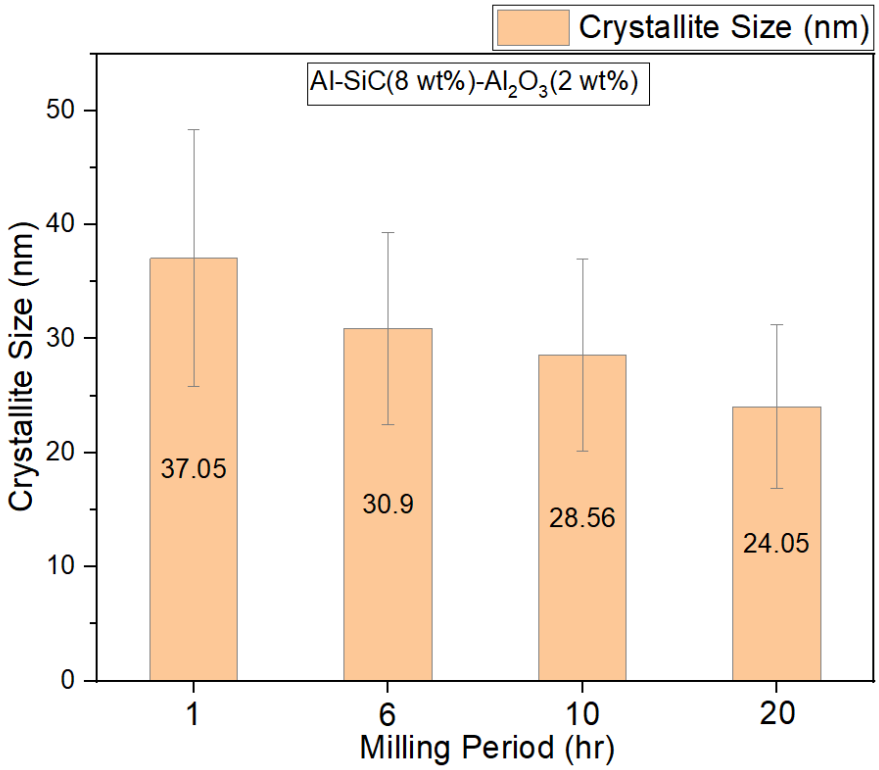

Figure 5.2(a): Results for crystallite size of composite powders after 1h, 6hr, 10 hr and 20 hr of mechanical milling for composite-1.

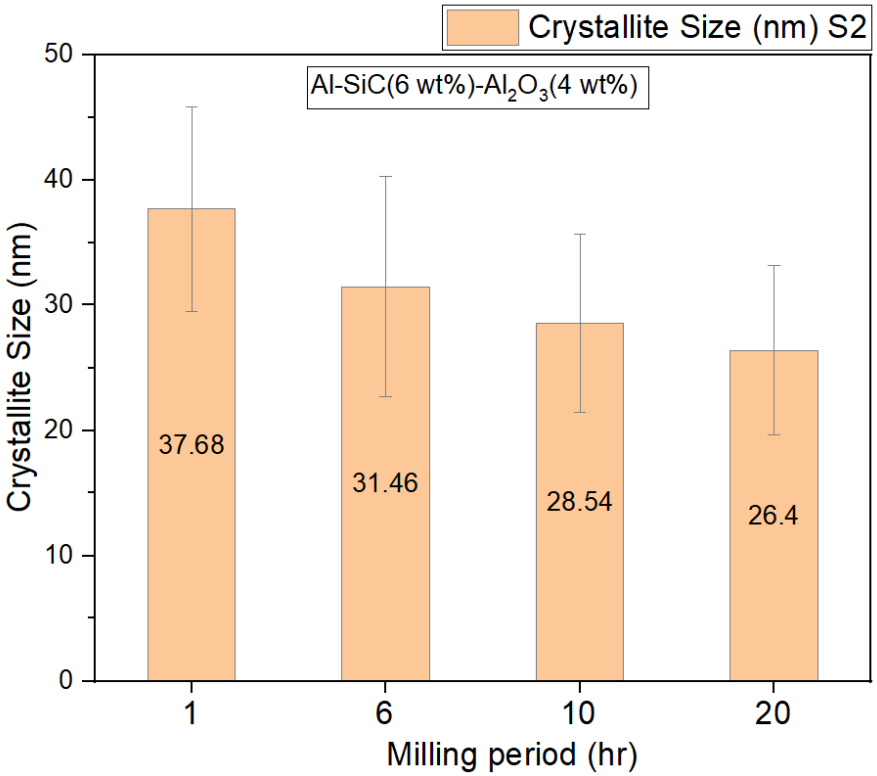

Figure 5.2(b): Results for crystallite size of composite powders after 1h, 6hr, 10 hr and 20 hr of mechanical milling for composite-2.

From the results based on Scherrer equation as shown in figure 5.2, slope of the curve is steep as compared to later stages of milling. During the milling process, crystallite size of 37 nm of crystallite size after 1hr, has reduced to approximately 25 nm after 20 hr for both of the compositions. Reduction of slope of the curve is due to the logarithmic change in crystallite size. Higher reduction in crystallite size of the composite with higher percentage of SiC is because of the reason that refinement increases with hardness of reinforcement particles due to the interaction of dislocations with tough reinforcing particles [20].

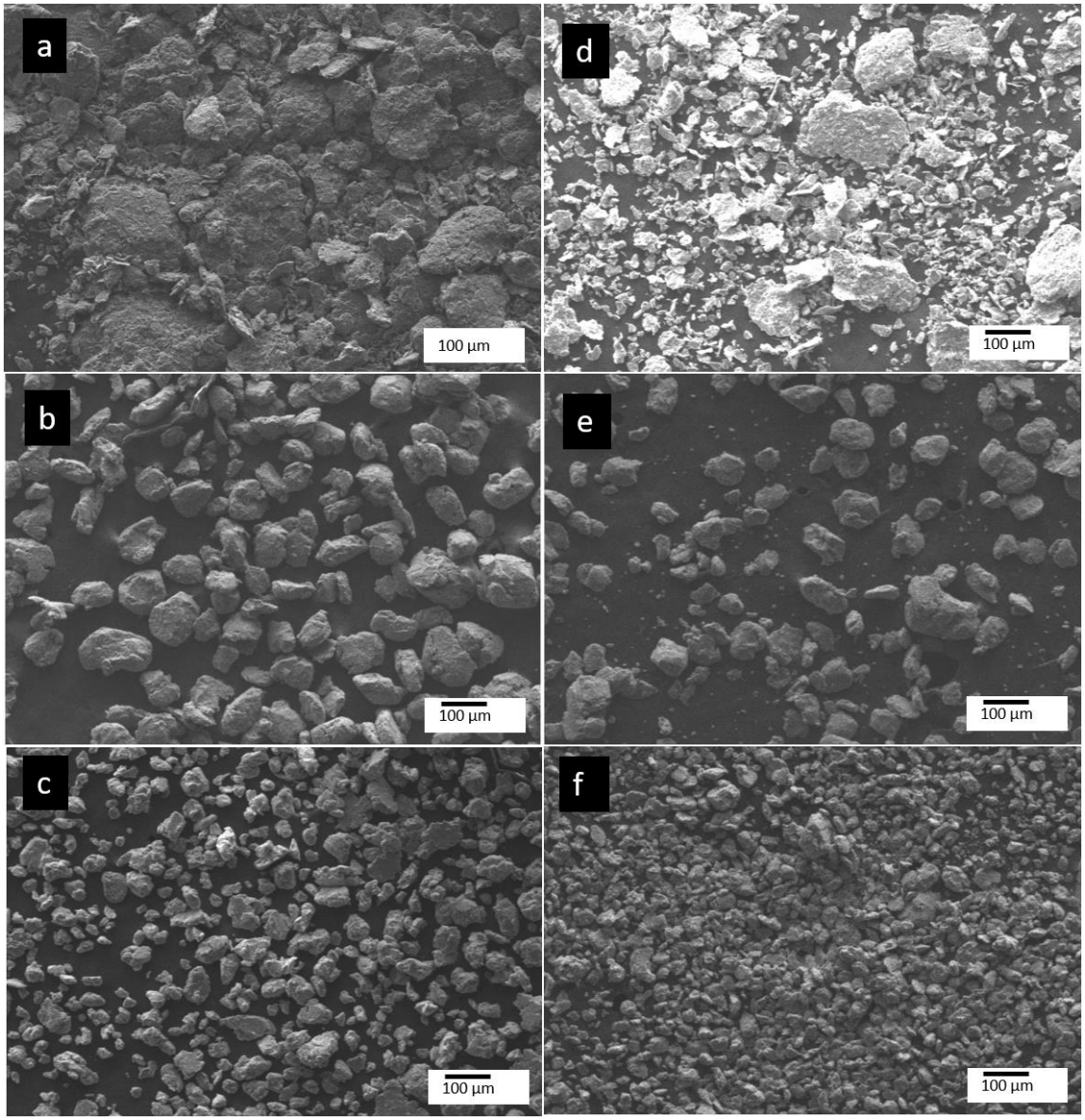

Figure 5.3: SEM images of 1h, 10h and 20h milled (a,b and c) Al-SiC 8 wt%-Al_2O_3 2 wt% and (d,e and f) Al-SiC 6 wt%-Al_2O_3 4 wt% powders.

Particle Sizes(in microns):

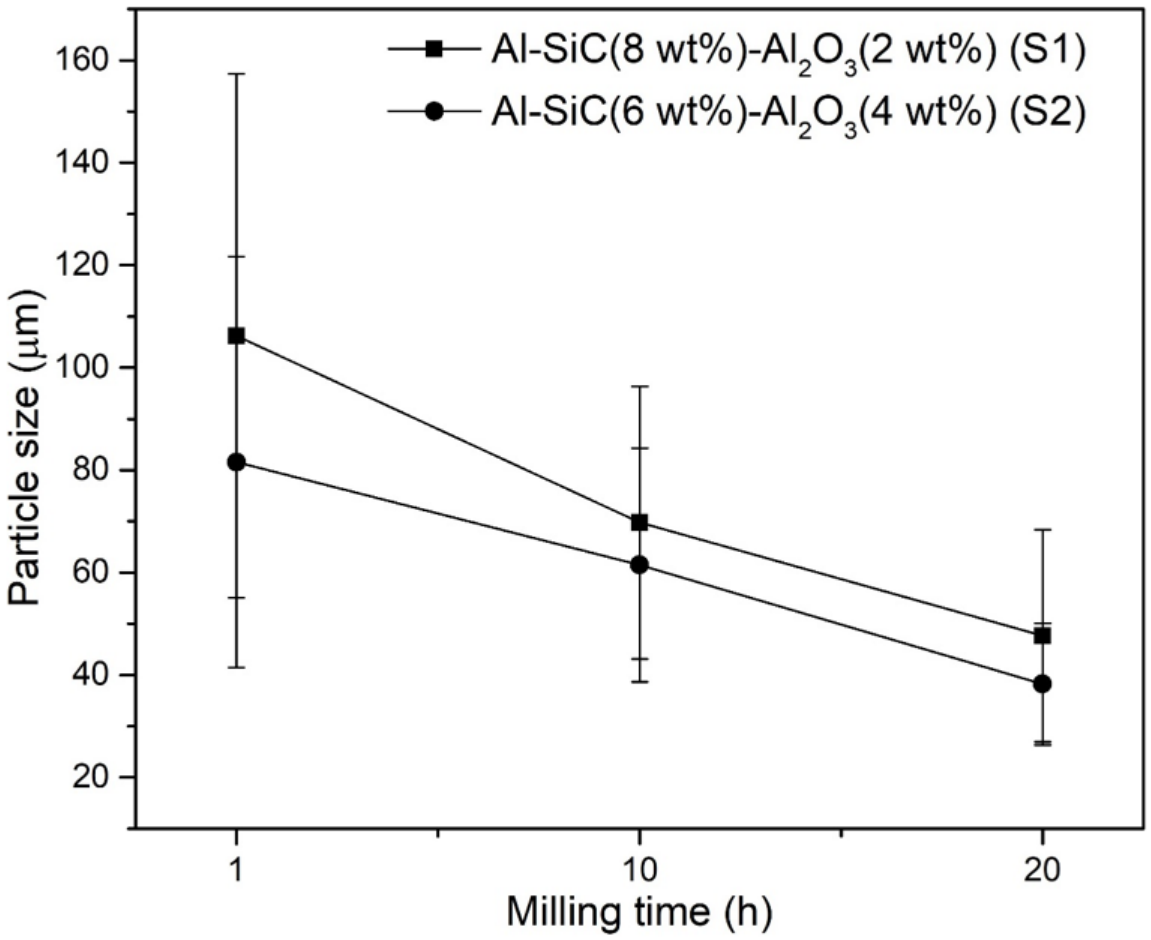

Figure 5.4: Results for particles size of composite powders after 1hr, 10 hr and 20 hr of mechanical milling.

In the early stage of 1 hr milling, large flattened particles (more than three times the size of initial particle size) are formed as shown in figure 5.3a and 5.3d. Flattening of large flattened particles are due to the tendency of soft particles to weld together. With continuing deformation during milling for 10 and 20 hrs, particles get work hardened and fracture by a fatigue failure mechnaism, reducing the particles size lesser than 50 μm. as shown in fig. 5.4. Successful reduction in particles' size is of the reason that tendency to fracture predominates over cold welding.

5.2 Density of Sintered Samples:

The sintered sample's density was calculated by a hydrostatic balance using Archimedes' principle in deionized water at room temperature. Measurement for 5 times is done to ensure the accuracy of the measurement results, and then take the average value. The relative density of the samples was calculated from the formula,

$$RD = (SD / TD) \times 100\%$$

Where SD was the sintered density, RD was the relative density and TD was the theoretical density.

Table 5.1: Results of measurement of relative density of SPS sintered composites at

Composition	*Sample's Name*	*Holding Time*	*Temperature*	*Pressure*	*Relative Density*
(Al-SiC 8 wt%- Al_2O_3 2 wt%)	***S 1-10***	***10 min***	***550ºC***	***50 MPa***	***95.44%***
(Al-SiC 8 wt%- Al_2O_3 2 wt%)	***S 1-15***	***15 min***	***550ºC***	***50 MPa***	***98.09%***
(Al-SiC 6 wt%- Al_2O_3 4 wt%)	***S 2-10***	***10 min***	***550ºC***	***50 MPa***	***95.56%***
(Al-SiC 6 wt%- Al_2O_3 4 wt%)	***S 2-15***	***15 min***	***550ºC***	***50 MPa***	***97.31%***

550^{o} C and 50 MPa.

The table 5.1 mentioned above shows the relative density of Spark Plasma Sintered Samples for both composites based on the holding time. In the sintering process of all the four samples, the

temperature and pressure were maintained constant i.e., 550˚C and 50 MPa respectively. On further increasing the temperature at the same pressure of 50 MPa, localisation of heat was taking place which resulted in the melting of sample.

The maximum density of the sample for composite-1 was achieved with 10 min holding time. For both of the composites, with the increase in holding time density of samples was found to be increased. This is due to achievement of better particle bonding and elimination of porosities at higher holding time during consolidation.

5.3 Microstructure analysis of sintered bulk samples

5.3.1 XRD analysis of the Al-SiC-Al_2O_3 sintered bulk samples

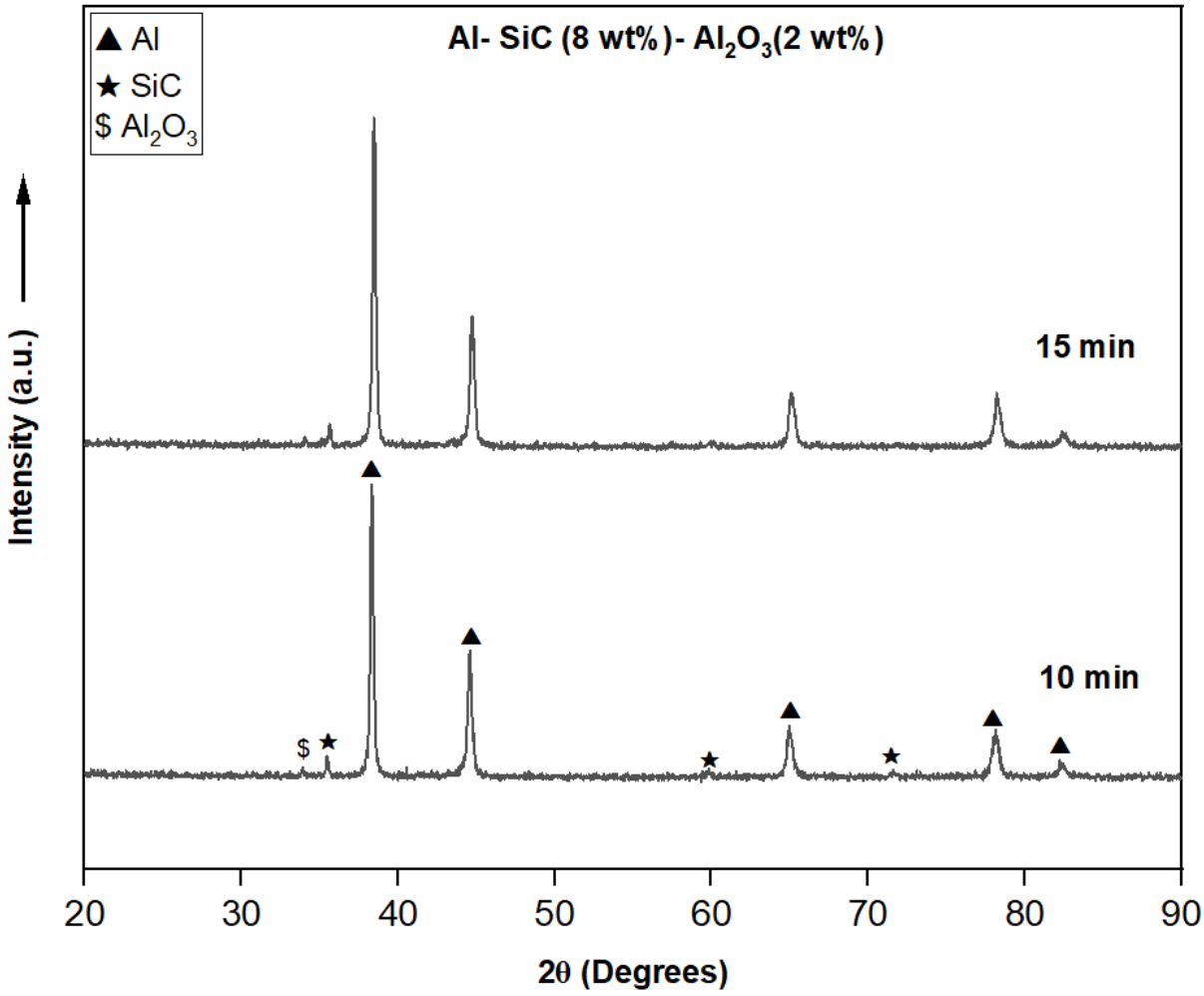

Figure 5.5: XRD patterns of SPS sintered composite 1 at different holding times. Al-SiC (8 wt%)-Al_2O_3 (2 wt%).

From fig. 5.5, fig. 5.6 and fig. 5.1, we can see the same peaks from the XRD pattern after the comparison of powders of composite 1, 2 and sintered samples. It shows during the sintering process, no new phases are formed, and regular Al, SiC, and Al_2O_3 phase are present in the studied composites.

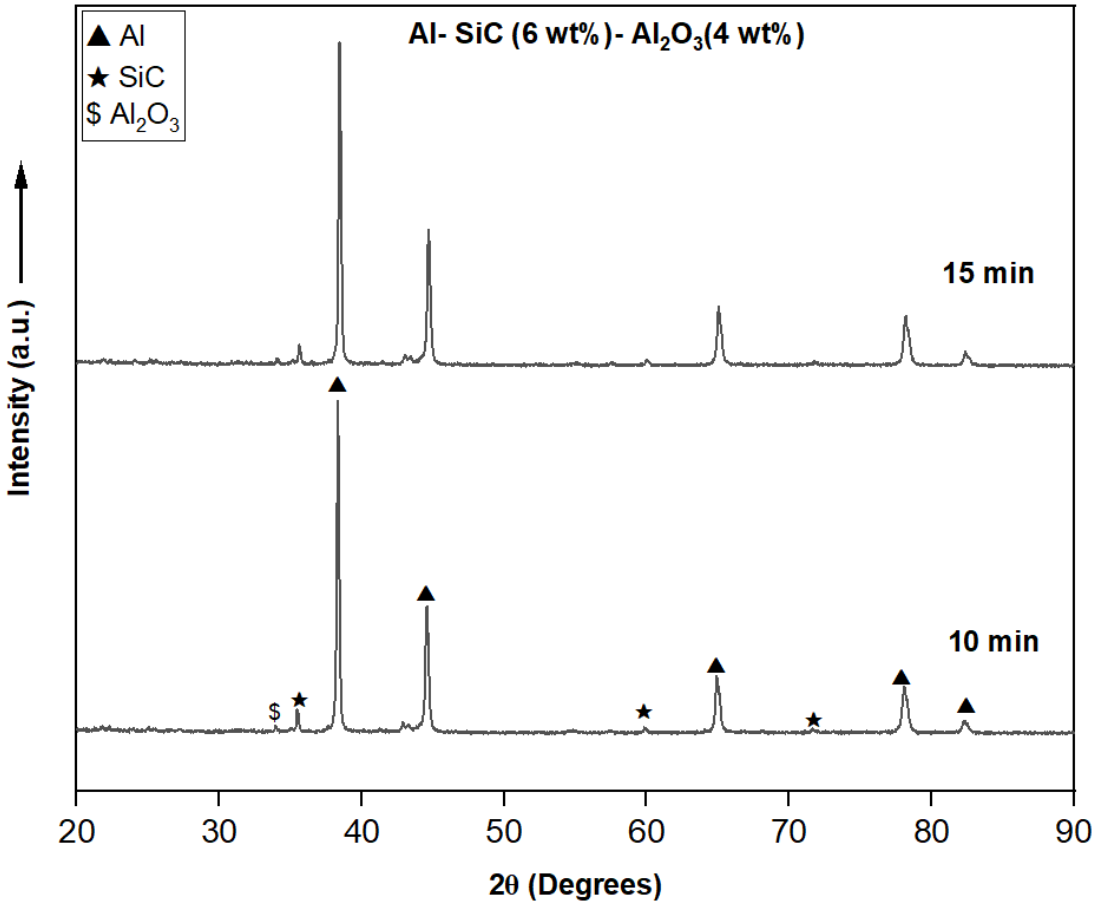

Figure 5.6: XRD patterns of SPS sintered composite 2 at different holding times. Al-SiC (6 wt%)-Al_2O_3 (4 wt%).

5.3.2 EDS Mapping of Composite Microstructures:

The below EDS mapping has been done with the help of a standard Scanning Electron Microscopy machine in order to find out the distribution of reinforcement particles in the metallic matrix. Homogeneous distribution is required to have the same strengthening effect due to reinforcement particles throughout the matrix on the application of load. Fig. 5.7 shows the homogeneous distribution of SiC and Al_2O_3 particles in the aluminium matrix. The red part of

the image shows the matrix material and green particles are SiC particles, and the bright part shows the alumina particles.

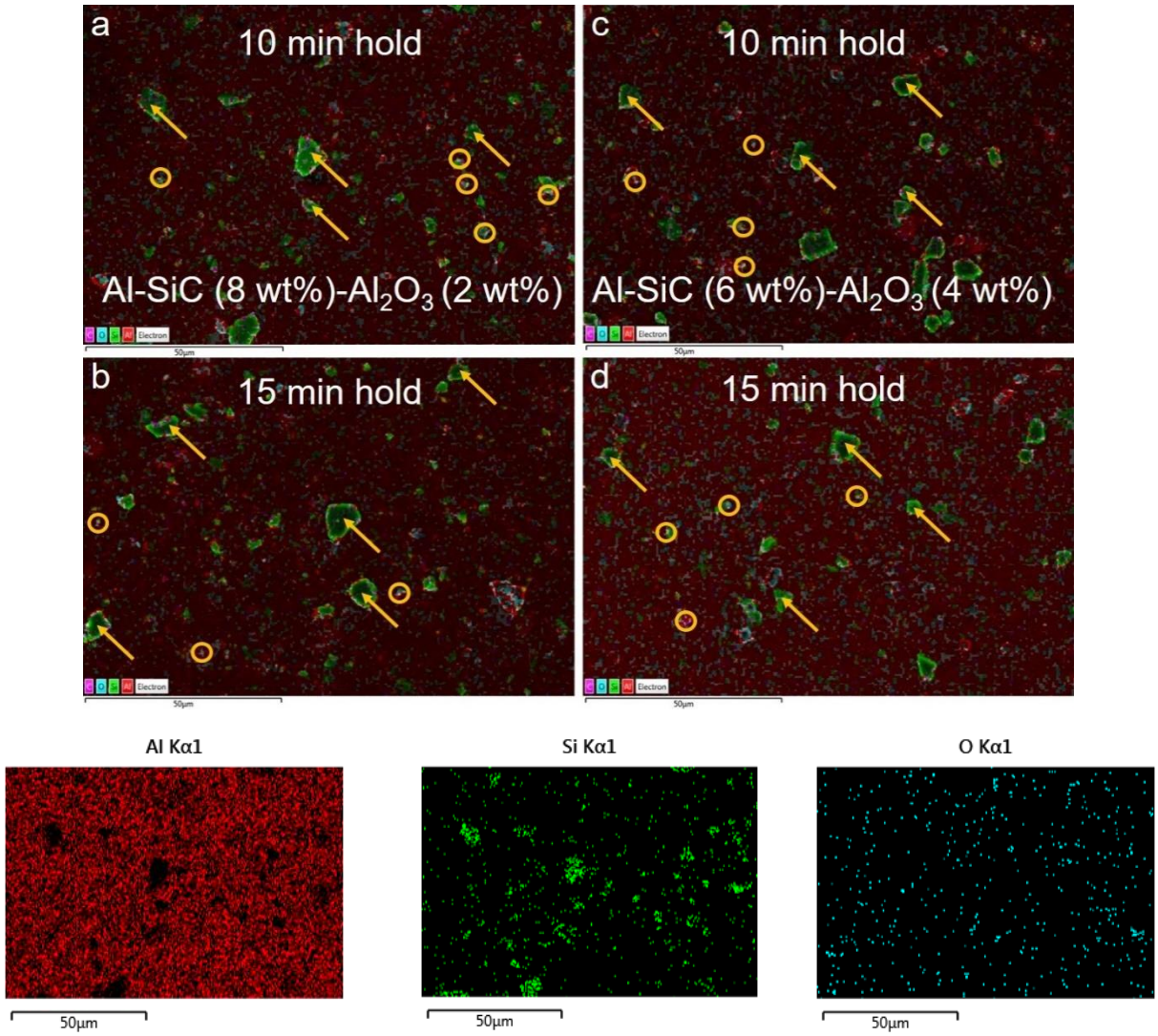

Figure 5.7: EDS mapping of SPS sintered composites depicting the distribution of reinforcement particles in the matrix.

5.3.3 SEM Images of Composite Microstructure:

Fig. 5.8 shows the SEM images of composite 1 (S 1-10, S 1-15) and composite 2 (S 2-10, S 2-15) at high magnification. Even at high magnification, it can be observed that there are no pores between the matrix and reinforcement particles and thus at the interface, a proper mechanical adhesion between the Al and reinforcement particles is observed.

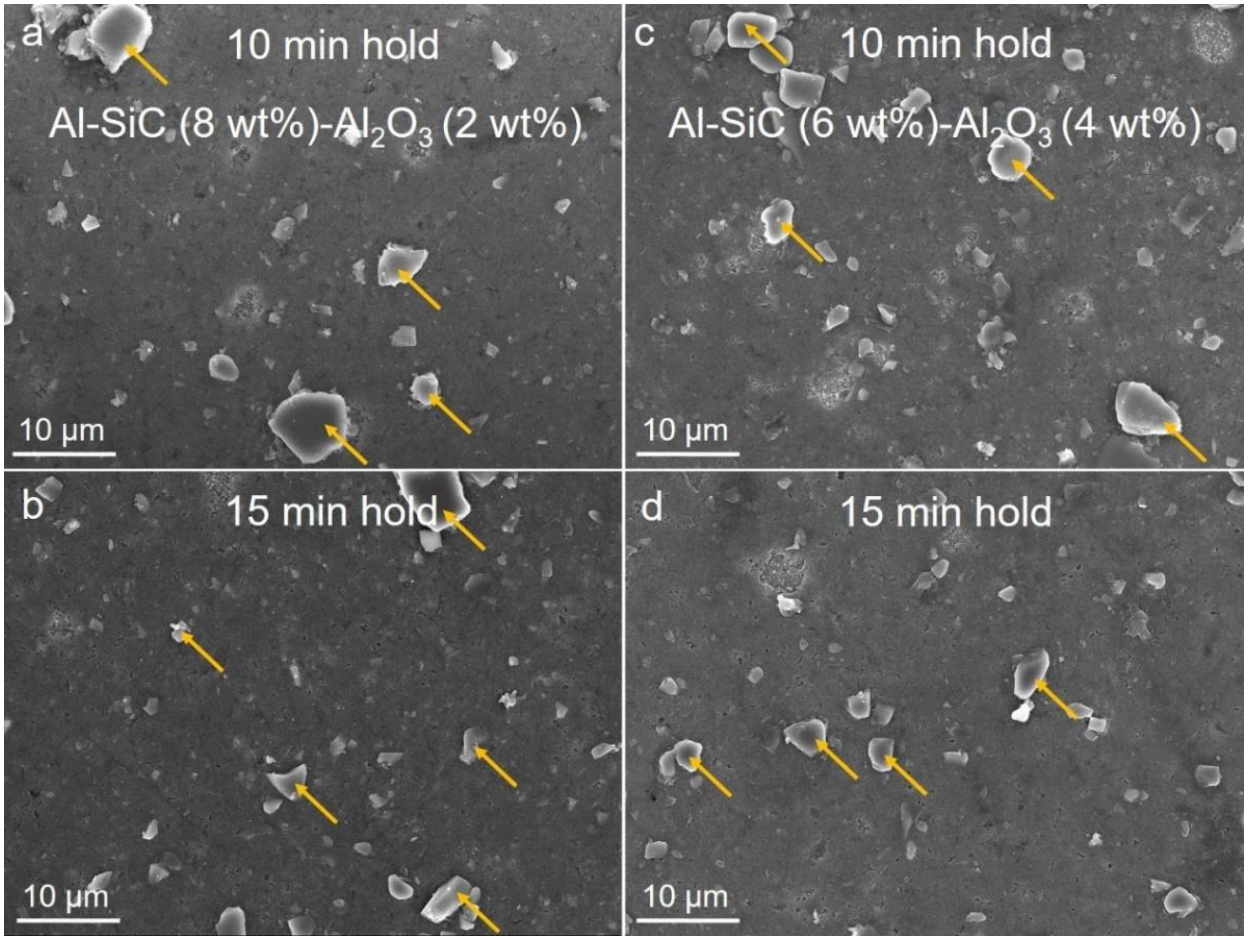

Figure 5.8: SEM images of the sintered samples consolidated from mechanically milled composite powders.

5.4 Mechanical Properties

5.4.1 Hardness

With the incorporation of the ceramic particles in the aluminium, hardness is increased by more than 150% as compared to unreinforced aluminium. The increase in hardness of the composites is attributed to the combination of the following strengthening mechanisms:

- Initial ball milling of powder particles imparts large deformation in them, leading to high dislocation density.
- Impedance of dislocation movement in the aluminium matrix through ceramic particles.

The maximum hardness was observed in the case of composite 1, where the percentage of SiC is more as compared to composite 2. The hardness values are also discussed in Fig. 5.9.

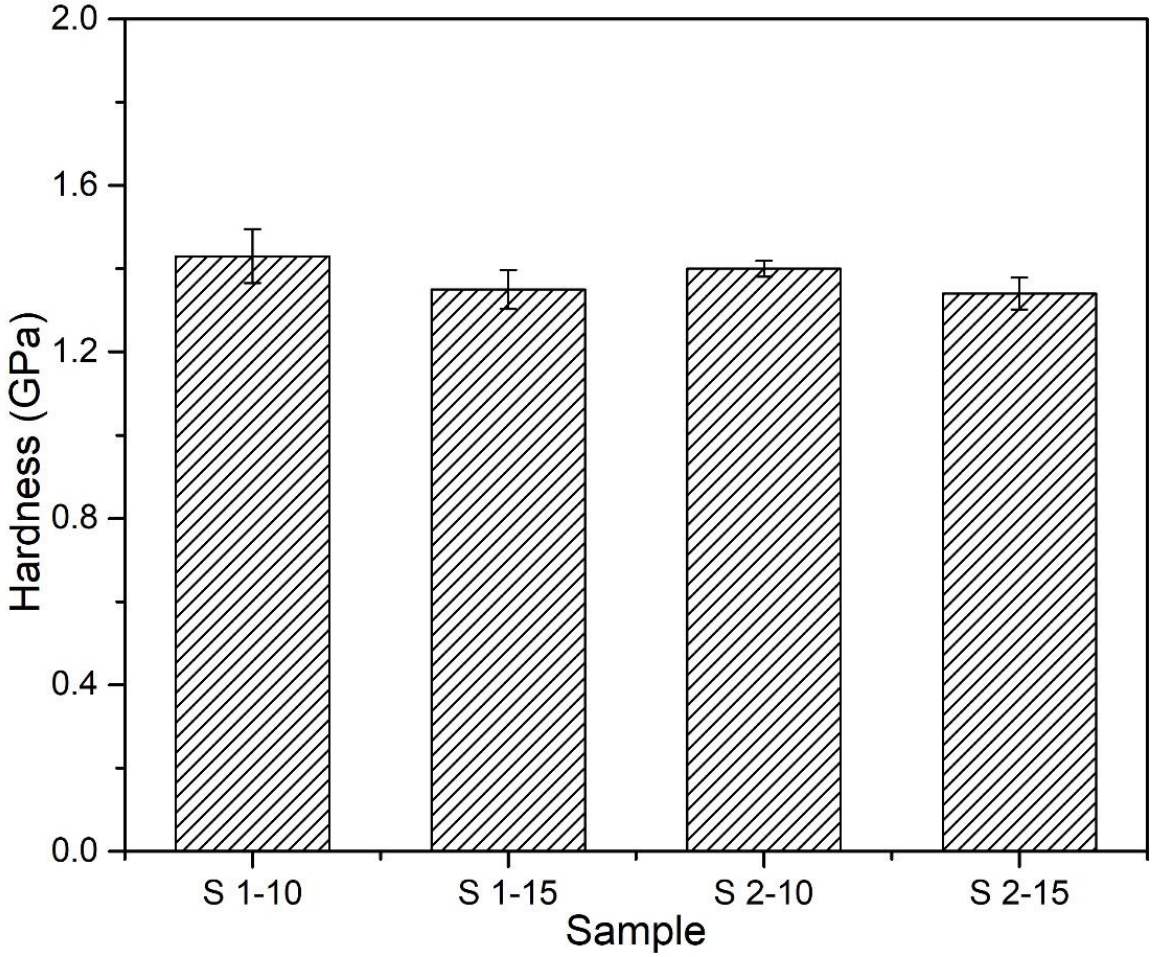

Figure 5.9: Micro hardness of the SPS sintered composite samples at 100 gf.

5.4.2 Fretting Wear

Fretting wear occurs at the surfaces which are subjected to high stresses at the surface along with the low amplitude of oscillations. Aluminium because of its unique property of lower density is utilized in many industries as aerospace, automotive, transportation and marine. Apart from improving the properties like hardness, tribological properties of materials is also of equivalent importance. During many applications, various body parts of aluminium are fastened with the help of rivet or bolt joints. As a result of these vibrations, these parts are subjected to relative movements of low amplitude between surfaces which further results in fretting wear damage of

surfaces. Due to removal of the oxide layers over the surface, it also lead to increased chances of corrosion, especially in marine applications.

For our research work, fretting wear is performed with the help of reciprocating fretting wear and tribocorrosion test machine along with using software, Win-Ducom 2010. The constant frequency and stroke of length are taken as 10 Hz and 200 micrometres respectively. The pin used as counter face material for fretting wear test is made of En31 steel of hardness 62 HRC, which is 6 mm diameter.

This test gave results of the coefficient of friction of samples. Stylus profilometer is used to measure the depth of scars of fretting wear test on each sample for different loads of 20N and 30N. SEM images are also taken to take measurements of scar to calculate wear volumes. Fig. 5.14 and Fig. 5.15 shows the data taken from stylus profilometer for each sample at 20N and 30 N respectively.

The equations mentioned below were used for the calculation of wear volume loss:

$$V = \frac{\Pi h^2}{3}(3R - h) \qquad \text{Equation (2)}$$

$$R = \frac{d_1 d_2}{8h} + \frac{h}{2} \qquad \text{Equation (3)}$$

Here, V = Wear Volume losses in mm^3

H = Wear Scar's Depth

R = Fretting area's radius of curvature

d1, d2 = fretting wear scar's length along the fretting direction and in the perpendicular direction.

Fig. 5.10 and 5.11 show the variation in coefficient of friction for samples at 20N and 30N, respectively, with an increase in the no. of cycles of fretting wear experiment at room temperature performed in dry conditions. The reason for sudden increase in the COF at the start of the test is because of the uneven surface and thus a steady state is achieved at later stages. Higher COF is observed in composite1 (Fig. 12(a, b), Fig.13 (a, b)) having higher percentage of SiC. Higher hardness of SiC as compared to Al_2O_3 results in better counteract with hard steel surface of pin of fretting wear machine and thus higher COF values are observed.

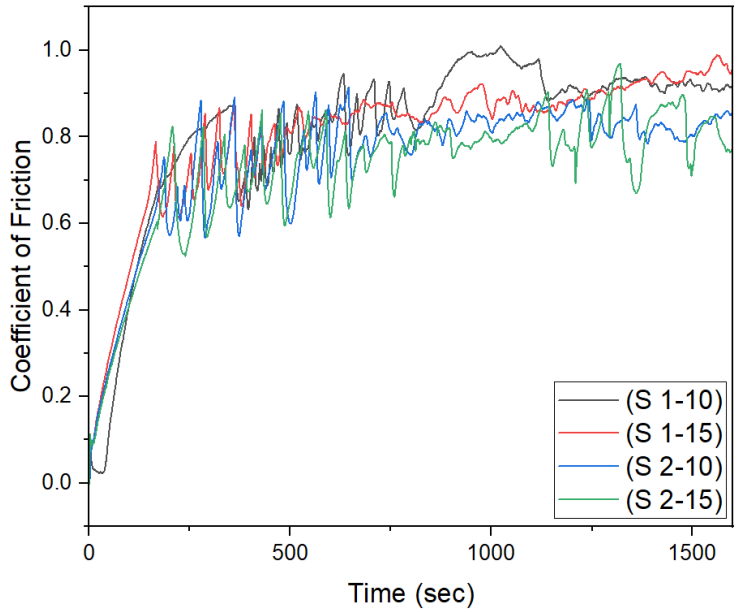

Figure 5.10: Variation of Coefficient of friction with number of fretting cycles for different sintered composites at applied load of 20N.

With the increase in loading conditions, it was observed that the coefficient of friction was reduced for each sample. This decrease in COF can be understood due to the formation of MML (mechanically mixed layers) of soft aluminium matrix and hard ceramic particles of SiC and Al_2O_3.

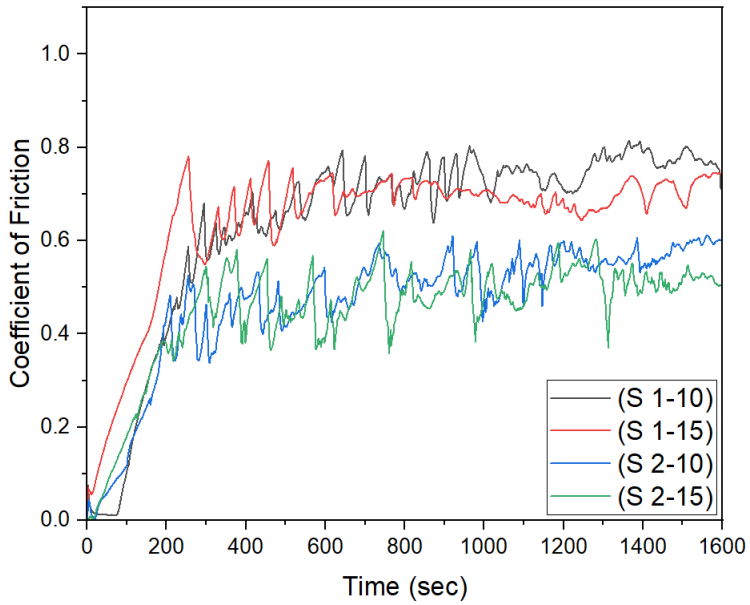

Figure 5.11: Variation of Coefficient of friction with number of fretting cycles for different sintered composites at applied load of 30N.

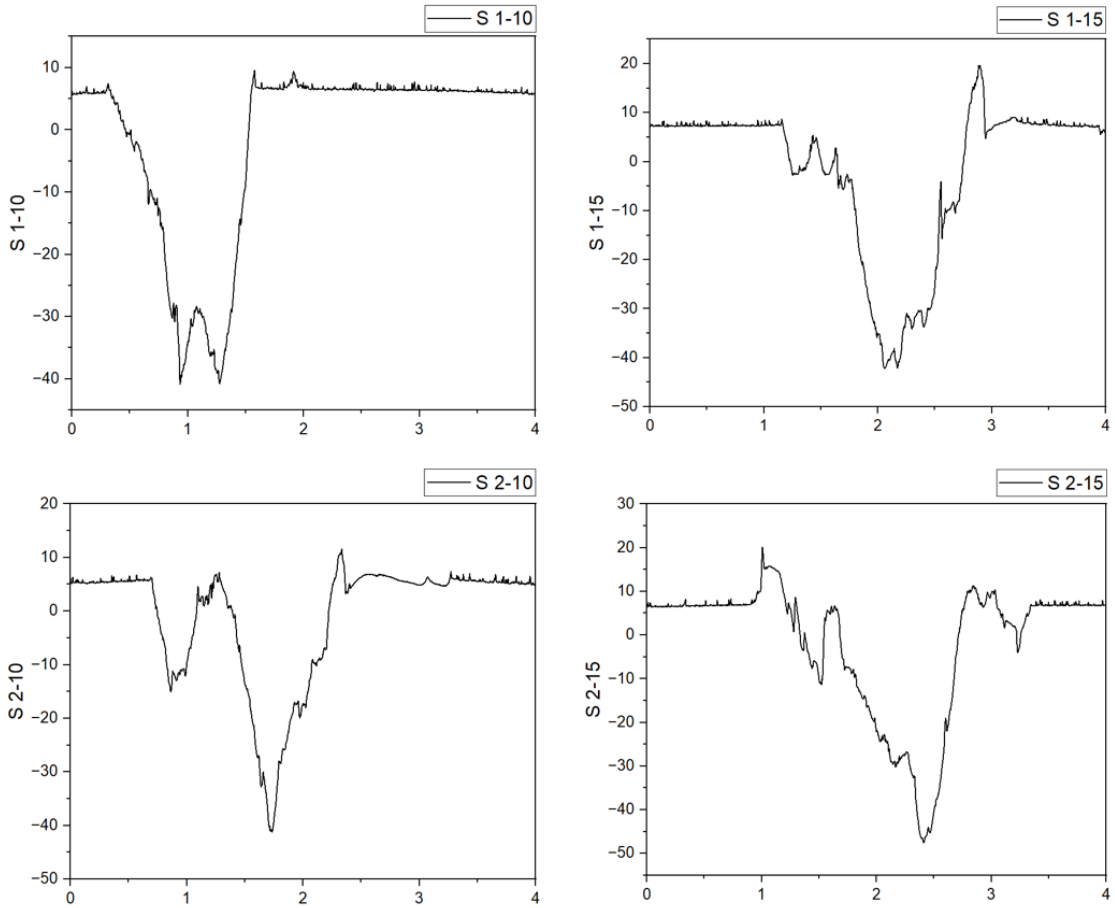

Fig. 5.12: Wear Scar depth profiles of the fretted composites at the applied load of 20N.

From the profile of fretting wear scars and their maximum depth, it was observed that they are not of exact “U” shape in contrary to the profile of unreinforced aluminium and the maximum depth is around 40 microns as compared to 110 microns in unreinforced aluminium discussed in other research works.

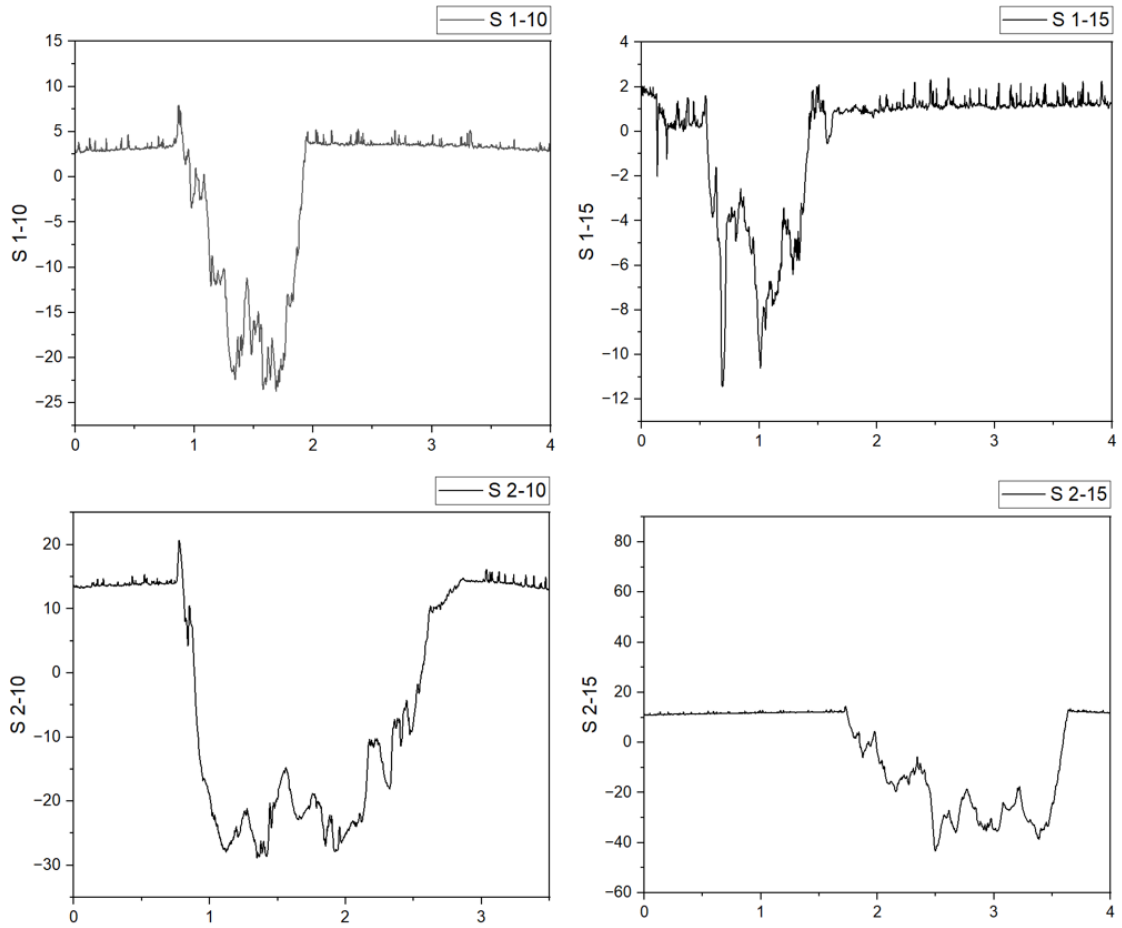

Figure 5.13: Wear Scar depth profiles of the fretted composites at the applied load of 30N.

Maximum wear volume loss was observed in the case of composite 2 (Al-SiC (6%) - Al_2O_3 (4%) 10 min, Al-SiC (6%) - Al_2O_3 (4%) 15 min) at higher loads. While in the case of composite 1, with an increase in load from 20N to 30N, a decrease in wear volume loss was observed.

The formation of MML check the transfer of the material from the surface and wear remains mild which is evident in the form of reduced wear rate in case of composite 1 (S 1-10, S 1-15). On the contrary, if cracking of MML takes place at higher load, it can also result in third body abrasion and higher wear rate is observed at higher load. Same phenomena may be possible in case of composite 2 (S 2-10, S 2-15), where higher wear volume losses are observed at higher loading conditions.

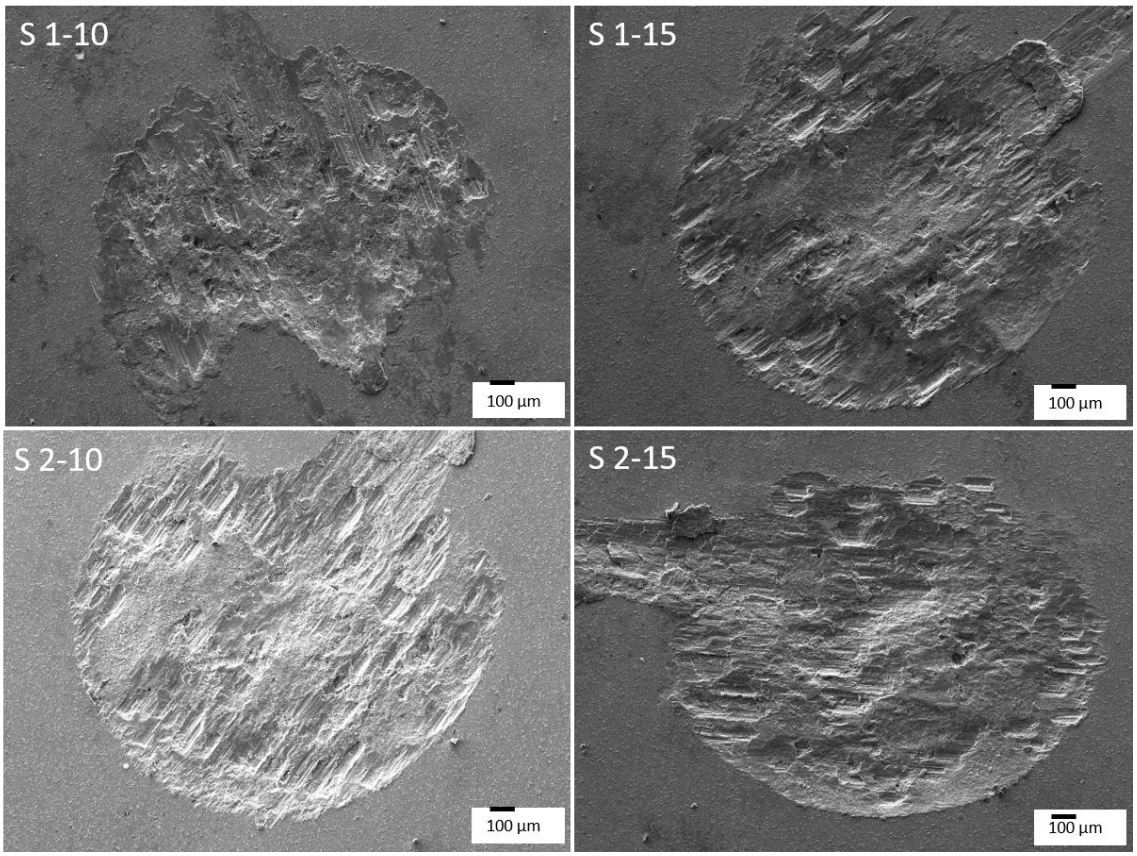

Figure 5.14: Wear Scar morphology of fretted composite samples at applied load of 20N.

Thus, composite 1 has better wear resistance properties in comparison with the other chosen composite. Also, it has far better wear resistance as compared to unreinforced aluminium metal too.

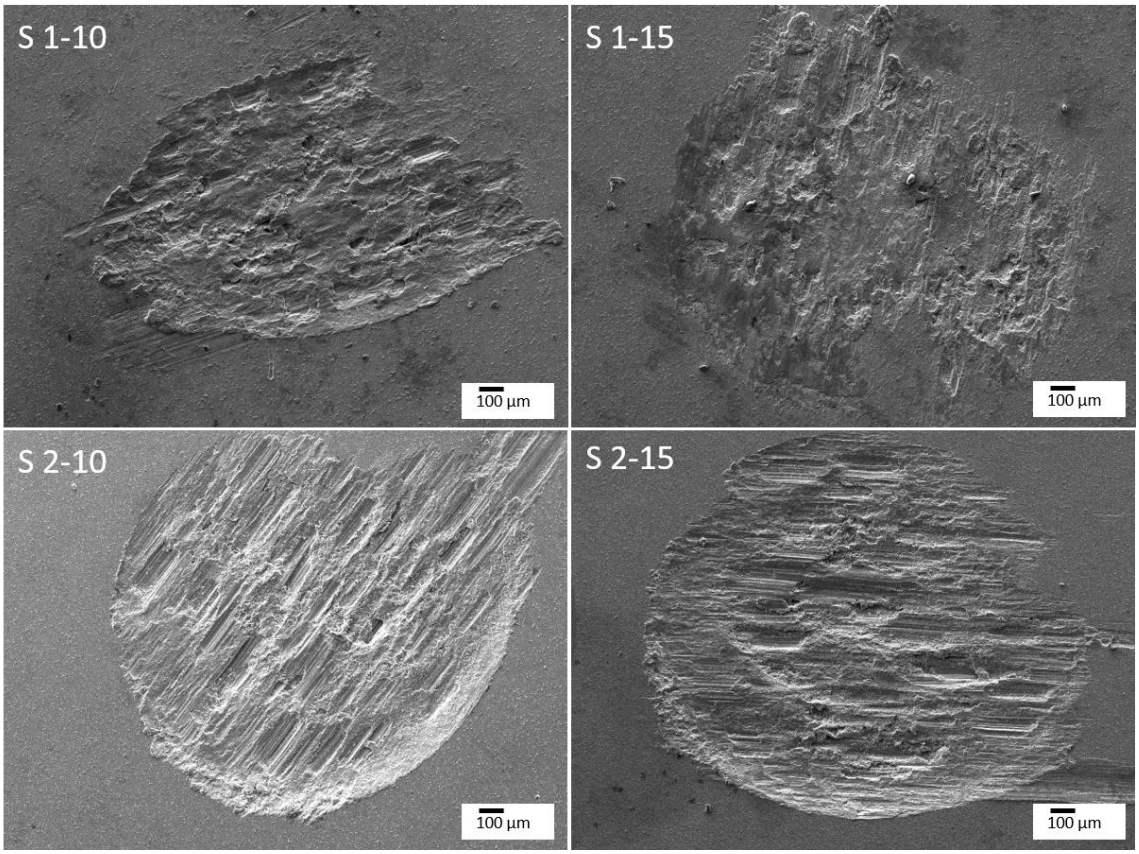

Figure 5.15: Wear Scar morphology of fretted composite samples at applied load of 30N.

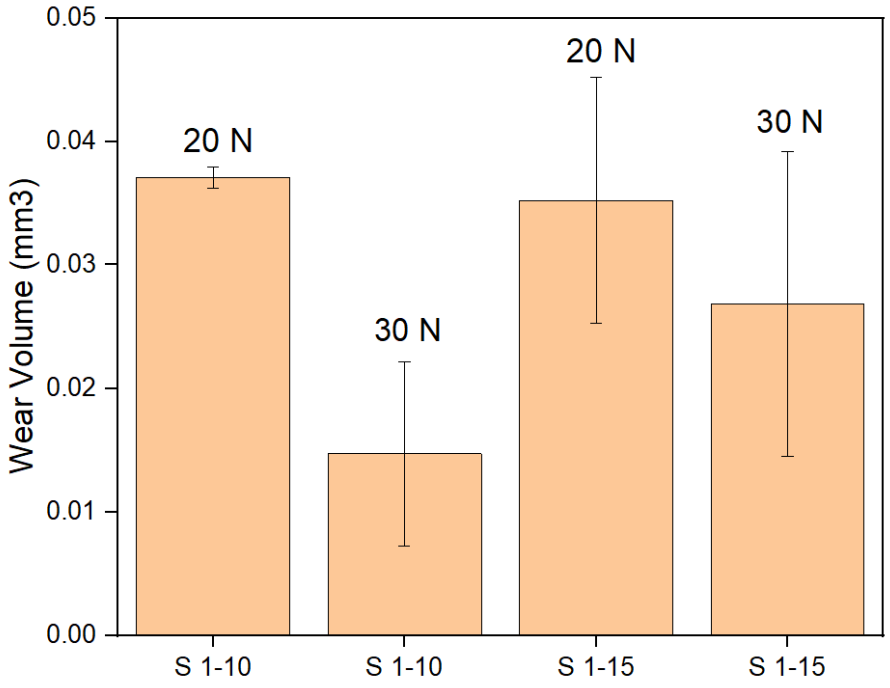

Figure 5.16: Wear volume loss of composite samples after fretting wear tests at applied load of 20 N.

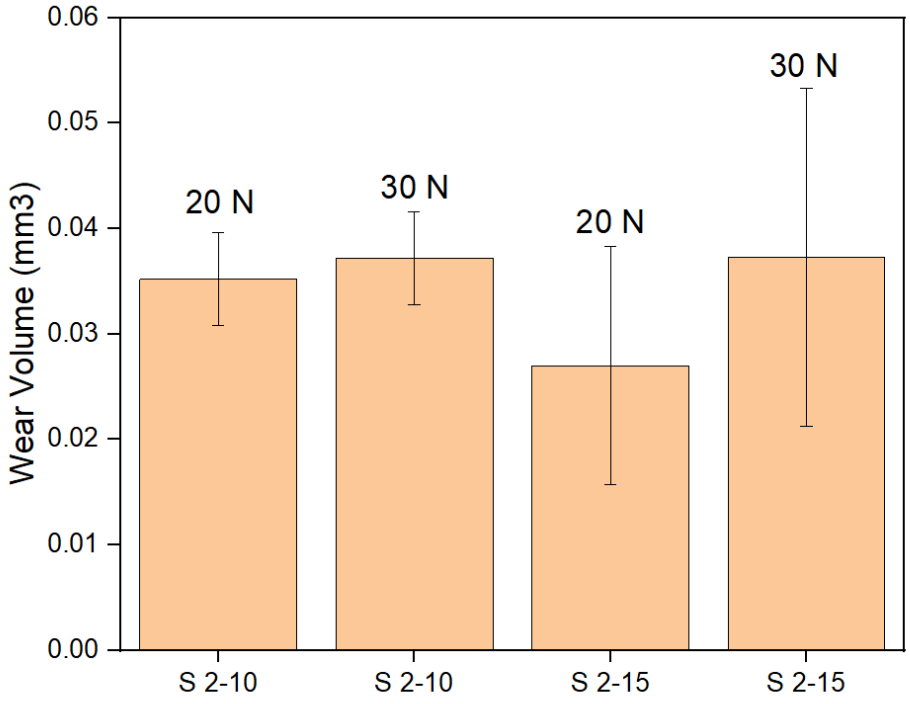

Figure 5.17: Wear volume loss of composite samples after fretting wear tests at applied load of 30 N.

5.4.3 Compression Test

Compression tests were carried out over the cylindrical specimens on a micro UTM machine, Shimadzu AGX-V2 under quasi-static conditions. Diameter of the cylindrical samples were 2.8 mm and a (l/d) ratio of 1.75 is maintained during the compression test at a strain rate of 5 x $10^{(-4)}$/s and thus the input for feed rate of the compression test were taken as 0.15 mm/min. The stress- strain curves of the Hybrid Aluminium Composites with different weight percentages of SiC and Al_2O_3 and with different holding time is shown in the fig. 5.17.

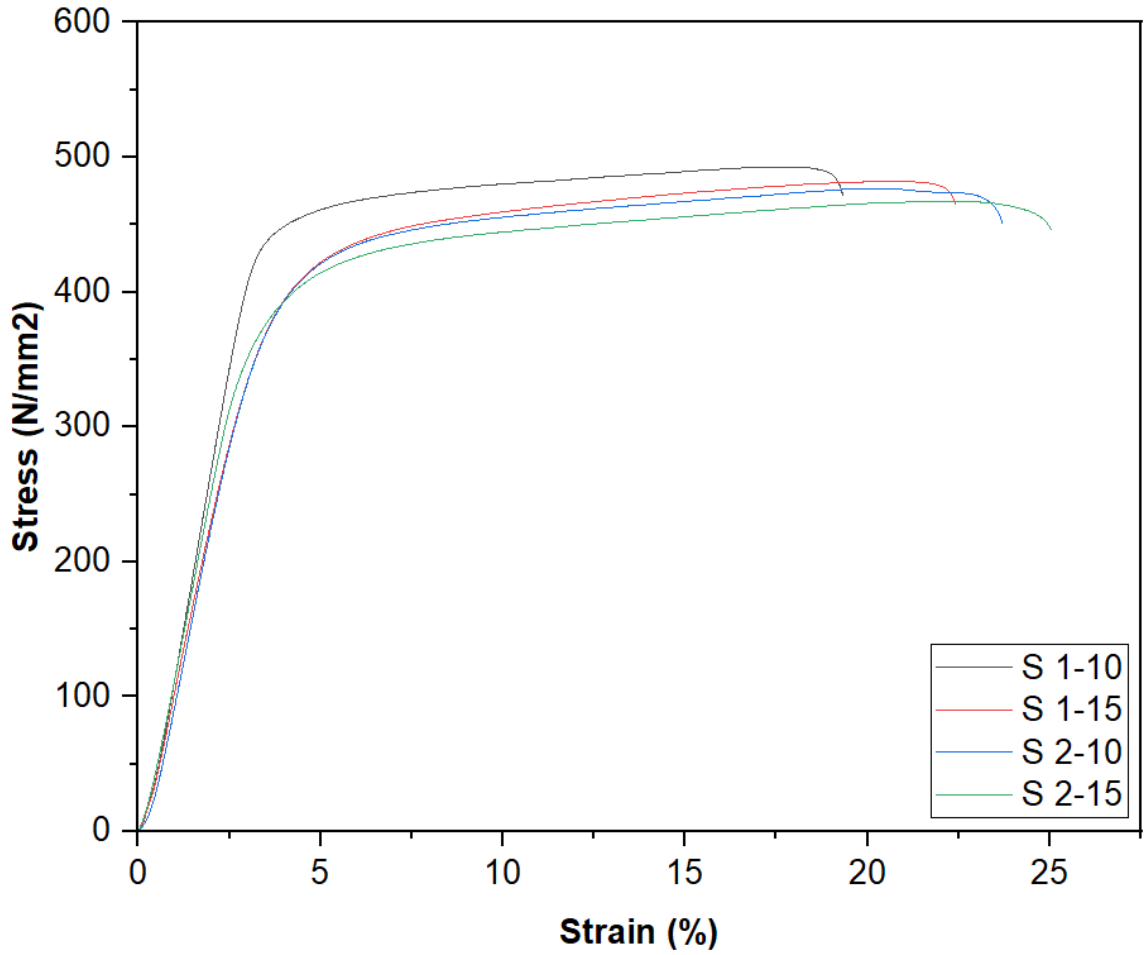

Figure 5.18: Stress Strain Curves of SPS sintered Aluminium metal matrix composites.

From the stress-strain curves, it can be pointed out that the strength and ductility follows the opposite trend. Composites with high wt% of SiC is having more strength compared to second chosen composition. Also along with more holding time, higher ductility is observed in both of the composites (S1 and S2). The strength of the chosen composites are found to be higher than pure aluminium (170 MPa) and the other aluminium alloys series, for e.g. Al 6XXX.

The reason for the better strength of the composites is the presence of SiC and Al_2O_3 in the aluminium matrix and the proper mechanical bonding between reinforcement particles and the matrix at the interface as shown in the SEM images in fig. 5.10. This leads to transfer of stress from the matrix to the particles. Also, there is difference in the coefficient of thermal expansion of ceramic particles (SiC and Al_2O_3) and matrix material (Al), this gives rise to thermal stresses in the material resulting in higher dislocation density in the material.

Table 5.2: Compression Strengths of SPS sintered composites.

Composite	Ultimate Compressive Strength (MPa)
S 1-10	492
S 1-15	482
S 2-10	476
S 2-15	467

Chapter 6

Conclusion and Future Scope

The present research work is based on successful investigations of strength improvement using ball milling and spark plasma sintering process and fabrication of aluminium composites to improve the tribological and mechanical properties for various automotive and aerospace applications.

By optimising parameters and changing the weight percentage of reinforcement, a powder metallurgy route was adopted to manufacture hybrid aluminium matrix composites. Energy Dispersive Spectroscopy (EDS), mechanical properties (hardness, compressive strength), and fretting wear behaviour were studied.

6.1 Conclusions

The following conclusions of the current work can be drawn with the help of analysis based on SEM images, XRD patterns, mechanical properties, and fretting behaviour of SiC and Al_2O_3 reinforced composites.

- Powder Metallurgy route (Ball milling and SPS sintering) can be successfully utilized to fabricate highly dense composites with superior tribological and mechanical properties.
- SEM micrographs of the polished composite's surface revealed the homogeneous distribution of reinforcement particles (SiC and Al_2O_3) in the aluminium matrix.
- XRD results revealed that no new phases were formed during the ball milling and sintering process as the temperature was maintained below the melting point.
- With the addition of different combinations of 10% reinforcement particles consisting of SiC and Al_2O_3, the hardness of composites was much higher compared to pure aluminium. An increase in hardness was observed with a higher percentage of SiC.
- Compression strength experiments on the synthesised composites (492 MPa) revealed an increment in the strength values by more than 200% as compared to aluminium (170 MPa).
- Coefficient of friction values were approximately 1 for the synthesised hybrid AMMCs and it decreased with an increase in the applied load.

- Wear volume losses were calculated based on the fretting wear scars over the surface generated during the test. The wear volume losses were lesser as compared to unreinforced aluminium.

The SPS Sintering process after the mechanical milling process therefore have a high capability of producing hybrid composites of superior quality.

6.2 Future Scope

- Further optimisation of ball milling parameters and spark plasma sintering parameters can be done to improve various characteristics further.
- Composites with different compositions can be again manufactured by additive manufacturing route.
- Tribological and mechanical properties of additively manufactured composite can then be compared with SPS sintered composites.

References

[1] D. Garbiec et. al. (2015), Properties of Al-Al2O3 composites synthesised by spark plasma sintering method, Archives of Civil and Mechanical Engineering.(DOI: 10.1016/j.acme.2015.02.004)

[2] Chen H, Alpas AT. (1996), Wear of aluminium matrix composites reinforced with nickel-coated carbon fibres. Wear; 192: 186-98.(DOI: 10.1016/0043-1648(95)06795-7)

[3] Shercliff HR, Ashby MF. (1994), Design with metal matrix composites. Mater Sci Technol; 10: 443-51.(DOI: 10.1177/09544089211042114)

[4] X. Zhu, J. Yu, X. Wang (2012), Microstructure and properties of Al/Si/ SiC composites for electronic packaging, Transactions of Nonferrous Metals Society of China 22 (7) 1686–1692. (DOI: 10.1016/S1003-6326(11)61374-5)

[5] M. Rahimian, N. Parvin, N. Ehsani (2011), The effect of production parameters on microstructure and wear resistance of powder metallurgy Al–Al2O3 composite, Materials & Design 32 (2) 1031–1038.(DOI: 10.1016/j.matdes.2010.07.016)

[6] I. Sabirov, O. Kolednik, R.Z. Valiev, R. Pippan (2015), Acta Mater. 53 (2005) 4919-4930.(DOI: 10.1016/S1003-6326(15)63736-0)

[7] F. Ogawa, C. Masuda, Composites: Part A 71 84-94.(DOI: 10.1016/j.compositesa.2015.01.005)

[8] O. Guillon, J. Gonzalez-Julian, B. Dargatz, T. Kessel, G. Schierning, J. Rathel, M. Herrmann (2014), Adv. Eng. Mater. 16 830–849. (DOI: 10.1002/adem.201300409)

[9] X.P. Li, M. Yan, G. Ji, M. Qian (2013), J. Nanomater. 2013 1–6. (DOI: 10.1016/S1003-6326(11)61462-3)

[10] H. Kwon, M. Leparoux, A. Kawasaki (2014),, J. Mater. Sci. Technol., 30, pp. 736-742. (DOI: https://doi.org/10.1016/j.jmst.2014.03.003)

[11] J.H. Wu, H.L. Zhang, Y. Zhang, X.T. Wang, Mater. Des., 41 (2012), pp. 344-348. (DOI: 10.1016/j.msea.2014.10.015)

[12] J.T. Zhang, L.S. Liu, P.C. Zhai, Z.Y. Fu, Q.J. Zhang (2008), Mater. Lett., 62, pp. 443-446. (DOI: 10.1016/j.msea.2008.10.015)

[13] S. Bathula, R.C. Anandani, A. Dhar, A.K. Srivastava (2012), Mater. Sci. Eng. A 545 97-102. (DOI: 10.1016/j.msea.2012.02.095)

[14] Z.H. Zhang, F.C. Wang, J. Luo, S.K. Lee, L. Wang (2010), Mater. Sci. Eng. A 527 7235-7240. (DOI: 10.1016/j.msea.2010.07.043)

[15] J.T. Zhang, H.J. Shi, M.C. Cai, L.S. Liu, P.C. Zhai (2009), Mater. Sci. Eng. A, 527, pp. 218-224. (DOI: 10.1016/j.msea.2009.08.067)

[16] H. Kwon, M. Leparoux, A. Kawasaki (2014), J. Mater. Sci. Technol., 30, pp. 736-742. (DOI: 10.1016/j.jmst.2014.03.003)

[17] K. Dash, D. Chaira, B.C. Ray (2013),, Mater. Res. Bull., 48, pp. 2535-2542. (DOI: 10.1016/j.materresbull.2013.03.014)

[18] R. Vintila, A. Charest, R.A.L. Drew, M. Brochu (2011), Mater. Sci. Eng. A, 528, pp. 4395-4407. (DOI: 10.1016/j.msea.2011.02.079)

[19] E. Ghasali, A. Pakseresht, F. Safari-kooshali, M. Agheli, T. Ebadzadeh (2015), Mater. Sci. Eng. A, 627, pp. 27-30. (DOI: 10.1016/j.msea.2014.12.096)

[20] C. Suryanarayana (2011), Synthesis of nanocomposites by mechanical alloying, J. Alloys Compd. 509 S229-S234. (DOI: 10.1016/j.jallcom.2010.09.063)

[21] S. Bathula, R. Anandani, A. Dhar, A. Srivastava (2012), Synthesis and characterization of Al-alloy/SiCp nanocomposites employing high energy ball mill and spark plasma sintering, Adv. Mater. Res. 410 224-227. (DOI:.4028/www.scientific.net/AMR.410.224)

[22] X.P. Li, C.Y. Liu, M.Z. Ma, R.P. Liu (2016), Microstructures and mechanical properties of AA6061-SiC composites prepared through spark plasma sintering and hot rolling, Mater. Sci. Eng. 650 139-144. (DOI: 10.1016/j.msea.2015.10.015)

[23] Kommel, Lembit & Kimmari, Eduard. (2023). Investigations of Structure and Tribological Properties of the Lightweight c-BN-based. (DOI: 10.1016/S1003-6326(11)61784-5)

[24] Thandalam, Satish & Ramanathan, Subramanian & Sundarrajan, Shalini. (2015). Synthesis, microstructural and mechanical. (DOI: 10.1016/j.jmrt.2015.03.003)

[25] Khayal, Osama. (2019). MANUFACTURING AND PROCESSING OF COMPOSITE MATERIALS. (DOI: 10.13140/RG.2.2.30822.57928.)

[26] Tripathy, Aravind & Sarangi, Saroj Kumar & Chaubey, Anil. (2018). A review of solid state processes in manufacture of Functionally Graded Materials. International Journal of Engineering and Technology. 7. 1-5. (DOI: 10.14419/ijet.v7i4.39.23686).

[28] Ravikumar et.al (2019), International Journal of Applied Engineering Research ISSN 0973-4562 Volume 14, Number 8 pp. 1865-1869.